https://doi.org/10.5194/egusphere-2026-6858
Preprint. Discussion started: 12 November 2026
© Author(s) 2026. CC BY 4.0 License.

Geomorphic responses to sequential experimental floods in the lower Spöl River, Switzerland

Maha Sheikh[1,2], Samuel Wiesmann[3], Paolo Perona[4], Virginia Ruiz -Villanueva[1,2]

[1] Geomorphology, Natural Hazards and Risks Research Unit, Institute of Geography, University of Bern, Bern 3012, Switzerland
[2] Oeschger Centre for Climate Change Research, University of Bern, Bern 3012, Switzerland
[3] Swiss National Park, Zernez, 7530, Switzerland
[4] Hydraulic Constructions Platform (PL-LCH), Institute of Civil Engineering (IIC), Ecole polytechnique f´ed´erale de Lausanne (EPFL), Lausanne 1015, Switzerland

Correspondence to: Maha Sheikh (maha.sheikh@unibe.ch)

Abstract. Experimental floods are increasingly used to restore geomorphic processes in regulated rivers, yet their effectiveness is often evaluated using only ecological indicators and mostly after individual flood events, limiting understanding of cumulative channel adjustment and the key controls on geomorphic response. This study evaluates the geomorphic effectiveness of six sequential experimental floods between 2018 and 2024 in the lower Spöl River, Switzerland, using a multi-metric assessment of channel change derived from repeat high-resolution topographic surveys. Geomorphic responses were quantified using erosion, deposition areas and volumes, sediment budgets, channel widening, vertical reworking, bed surface grain size, roughness, and slope, and were examined in relation to flood hydrograph characteristics and the initial state of the channel. All floods reactivated geomorphic processes through sediment mobilisation, erosion, deposition and channel adjustment, but the magnitude and form of the response varied markedly among events. Total flood volume was a better, although not exclusive, predictor of sediment mobilization than peak discharge or flood duration, while antecedent channel conditions, including sediment availability, bed surface grain size, channel morphology, roughness, slope and the legacy of earlier events, strongly influenced the magnitude and spatial distribution of channel adjustment. Moreover, event-scale effectiveness did not determine the river's longer-term trajectory: despite repeated sediment mobilisation, continued sediment delivery from an unregulated tributary, the Ova da Cluozza, promoted multi-year sediment storage and aggradation. These findings show that geomorphic effectiveness emerges from the interaction between hydraulic forcing, sediment availability and evolving channel conditions, and depends on the temporal scale of assessment. The multi-event, multi-metric approach provides a transferable framework for designing and evaluating sediment-informed experimental floods in regulated gravel-bed rivers.

1 Introduction

Natural flood regimes play a fundamental role in maintaining the geomorphic and ecological functioning of river systems by driving sediment transport, channel adjustment, floodplain connectivity, and habitat renewal (Junk et al., 1989; Wohl, 2016).

https://doi.org/10.5194/egusphere-2026-6858
Preprint. Discussion started: 12 November 2026
© Author(s) 2026. CC BY 4.0 License.

The magnitude, frequency, duration, and timing of floods regulate the balance between erosion and deposition, sustain channel complexity, and create the dynamic disturbance regimes many aquatic and riparian ecosystems depend on. Periodic floods mobilize sediment, reshape gravel bars, prevent excessive vegetation encroachment, and maintain the lateral and longitudinal connectivity necessary for diverse and resilient river-floodplain environments (Junk et al., 1989; Wohl, 2016). Despite their importance, river regulation has extensively altered natural flood regimes. More than 62,000 large dams are currently registered worldwide (International Commission on Large Dams (ICOLD)), profoundly modifying downstream hydrological variability and geomorphic processes. River regulation through dam construction has altered fluvial systems worldwide by modifying the natural interactions between flow, sediment transport, and channel morphology (Kondolf and Swanson, 1993; Lane et al., 2022; Smith and Mohrig, 2017) Dams disrupt the longitudinal continuity of rivers by regulating discharge and trapping large volumes of sediment, thereby fundamentally altering both sediment supply and transport capacity downstream (Grant et al., 2003). These alterations frequently result in channel simplification (Ligon et al., 1995), channel incision (Kondolf and Swanson, 1993; Smith and Mohrig, 2017; Williams and Wolman, 1984) and bed armouring (Kondolf and Swanson, 1993). Dams may also promote channel narrowing, changes in river planform (Galay, 1983; Kondolf and Swanson, 1993), reduced lateral connectivity and declining morphological diversity downstream (Lane et al., 2022). Reduced sediment mobility and suppression of flood disturbances may also promote the accumulation of fine sediments within the channel bed. In gravel-bed rivers, decoupling flow and sediment regimes can substantially alter sediment transport pathways and reduce the geomorphic disturbances needed to maintain channel heterogeneity (Kondolf & Swanson, 1993). Consequently, many regulated rivers experience vegetation encroachment, sediment stabilization, and progressive loss of habitat and morphological diversity downstream (Graf, 2006; Mulligan et al., 2021; Poff and Zimmerman, 2010). These widespread impacts have led to the increasing use of the so-called environmental flood releases (here referred to experimental floods) as restoration measures aimed at partially re-establishing geomorphic activity and ecological functionality in regulated rivers (Loire et al., 2021). By reintroducing controlled high-flow disturbances downstream of dams, these releases aim to restore components of natural flow variability and reactivate physical processes suppressed under regulated conditions (Konrad et al., 2011; Magdaleno, 2017). Experimental floods can promote sediment entrainment, gravel-bar reworking, channel-bed mobilization, and increased habitat dynamism, thereby enhancing both geomorphic activity and ecological functioning (Bender et al., 2022; Olden et al., 2014). For example, in North America, controlled flood releases on the Colorado River downstream of Glen Canyon Dam have aimed to rebuild sandbars and improve aquatic habitats since (Patten et al., 2001), while the Trinity River restoration program has focused on sediment mobilization, gravel-bar rebuilding, and enhancement of channel complexity and floodplain connectivity (Gaeuman et al., 2017). In Australia, environmental flow programs in the Murray–Darling Basin and Snowy River systems have targeted wetland inundation, sediment transport, and riffle-pool morphology restoration (Bender et al., 2022; Kingsford et al., 2017). In Africa, controlled flood releases on the Senegal and Zambezi rivers have supported fisheries, agriculture, and floodplain productivity (Beilfuss, 2001). In Asia, a notable example comes from the Satsunai River in Hokkaidō, Japan, where artificial floods have been released from Satsunai River Dam since 2012 as part of a large-scale restoration experiment, with the aim of restoring gravel-bed habitat, reactivating former braided channels, reducing riparian forest encroachment, and

https://doi.org/10.5194/egusphere-2026-6858
Preprint. Discussion started: 12 November 2026
© Author(s) 2026. CC BY 4.0 License.

maintaining flood conveyance capacity (Sumitomo et al., 2018; Yamaguchi et al., 2016). In Europe, experimental floods have also been implemented for a range of geomorphic and ecological objectives. On the Ebro River in Spain, these floods have focused on flushing fine sediments and improving habitat conditions (Magdaleno, 2017).

In Switzerland, two major regulated rivers provide further examples of long-term experimental-flood programmes. Similarly, experimental flood programs have been implemented on two major rivers in Switzerland. A series of six experimental floods were released between 2016 and 2022 from Rossens Dam on the Sarine River, aiming to mobilize sediments and improve habitat heterogeneity (Essyad et al., 2024; Stähly et al., 2019). In comparison to this short-term program on Sarine River, experimental floods program on the Spöl River represents one of the longest running initiatives worldwide. Launched in 2000, floods have been generated through coordinated releases from the Punt dal Gall (Livigno) reservoir and the Ova Spin Dam, with the objectives of restoring sediment dynamics, increasing morphological heterogeneity, flushing fine sediments, and improving overall ecological integrity (Robinson et al., 2018; Scheurer & Molinari, 2003; Schläfli et al., 2018).

Collectively, these examples highlight both the global expansion of experimental flood programs and the diversity of geomorphic and ecological objectives associated with environmental flow restoration. Despite their increasing implementation, the geomorphic effectiveness of experimental floods remains highly variable among river systems and between flood events. While some studies report substantial channel adjustment and sediment redistribution following experimental releases, others demonstrate limited or short-lived responses due to constraints imposed by sediment availability, initial channel conditions, and tributary inputs (Lisle and Church, 2002; Madej et al., 2009). In many regulated gravel-bed rivers, restoring flow disturbance alone may be insufficient to recover long-term geomorphic dynamics when dams disrupt sediment continuity (Stähly et al., 2019). Consequently, understanding how repeated flood releases interact with evolving channel conditions and external sediment supply has become a major challenge in river restoration and environmental flow management.

Despite more than two decades of research on the Spöl experimental flood program in Switzerland, most studies have focused primarily on ecological responses (Finch et al., 2025; O'Callaghan et al., 2025) or short-term geomorphic effects of individual flood releases. Consequently, the river's cumulative geomorphic adjustment to sequential experimental floods and the long-term geomorphic effectiveness of these floods remain poorly understood. Furthermore, long-term geomorphic monitoring has largely focused on the upper Spöl, immediately downstream of the Punt dal Gall Dam, whereas the lower Spöl (downstream of the Ova Spin Dam) has received comparatively little attention. Although the objectives of experimental flood releases were clearly defined for the upper Spöl River (Scheurer & Molinari, 2003), their geomorphic implications for the lower Spöl River remain less explicitly articulated, making it difficult to evaluate whether repeated flood releases have achieved meaningful morphological adjustment within this downstream reach. Existing studies in the lower Spöl have mainly investigated the effects of one or two individual flood events (Consoli et al., 2022; Hashemi et al., 2024; Robinson et al., 2018; Ruiz-Villanueva et al., 2022; Soto Parra et al., 2024). Only one study covers a similar time period, but it explored only the effects of experimental floods on sediment grain size (Ruiz-Villanueva et al., 2026). Although these studies provide valuable insights into event-scale

https://doi.org/10.5194/egusphere-2026-6858
Preprint. Discussion started: 12 November 2026
© Author(s) 2026. CC BY 4.0 License.

responses, they do not capture the longer-term morphological trajectory of the river under repeated experimental flood releases, nor do they address cumulative adjustments in sediment balance, channel planform, and surface structure.

In addition, the role of flood hydrological characteristics and initial channel conditions in shaping geomorphic response remains largely unexplored. Addressing these questions is critical for understanding whether experimental flood programs can effectively drive sustained geomorphic rehabilitation in regulated rivers. This study provides the first multi-year geomorphic assessment of sequential experimental floods in the lower Spöl River.

Specifically, the study aims to evaluate the effectiveness of experimental floods in the lower Spol by: (i) quantifying reach- and sub-reach-scale patterns of aggradation, degradation, and net sediment balance before and after each flood; (ii) evaluating pre- and post-flood channel planform adjustments and long-term trends in active channel width and cross-sectional geometry; (iii) assessing changes in surface roughness and channel slope as indicators of morphological heterogeneity; (iv) examining the relationship between flood hydrological characteristics and observed geomorphic responses in order to identify the key factors controlling river adjustment to sequential experimental floods; and (v) evaluating the role of initial conditions of the channel including the pre flood grain size and slope in shaping the geomorphic response of rivers to floods.

2 Study Area and the Experimental Flood Program

The Spöl River catchment (295 km²) is a tributary of the Inn River within the Danube River Basin and is located in the central Alps along the border between Switzerland and Italy. The catchment extends across northern Italy and the Canton of Graubünden in eastern Switzerland, with more than 80% of its area protected within the Swiss National Park and the Stelvio National Park. The river originates at the Forcola di Livigno in Italy at an elevation of approximately 2315 m.a.s.l. and consists of two regulated sections controlled by the Punt dal Gall (Livigno) and Ova Spin reservoirs, which were constructed during hydropower development in the 1960s. Regulation substantially altered the natural flow regime of the river, reducing downstream residual discharge to approximately 0.9–1.0 m³/s compared to pre-dam mean annual flows of 6.6–12.5 m³/s and natural peak floods ranging from 36 to 140 m³/s (Scheurer & Molinari, 2003). These hydrological alterations resulted in pronounced geomorphic and ecological degradation downstream, including reduced sediment mobility, channel stabilization, and habitat simplification.

To mitigate these impacts, the Swiss National Park (SNP), the hydropower company Engadiner Kraftwerke (EKW), and cantonal and federal authorities initiated an experimental flood program in 2000. Since then, twenty-three experimental floods have been released from the Ova Spin Dam (as of June 2025), typically once or twice per year depending on water availability and management objectives. Flood magnitudes generally range between 15 and 25 $m^3 s^{-1}$ (approximately a 1-year recurrence interval) and 30 and 40 $m^3 s^{-1}$ (approximately a 10-year recurrence interval). Unlike sediment-flushing flows, these releases originate from the upper outlets of the dam and therefore contribute little sediment to the downstream channel. Instead, they primarily mobilize, redistribute, and rework sediment already present within the river system. The present study focuses on the geomorphic response to the seven experimental floods released between 2018 and 2024.

https://doi.org/10.5194/egusphere-2026-6858
Preprint. Discussion started: 12 November 2026
© Author(s) 2026. CC BY 4.0 License.

This study focuses on the lower Spöl River downstream of the Ova Spin reservoir, where the unregulated tributary Ova da Cluozza enters the main channel approximately 3.5 km below the dam (Figure 1). The Ova da Cluozza contributes approximately 0.2–0.8 m^3/s during baseflow conditions and up to ~12 m^3/s during snowmelt and rainfall events (FOEN, 2024). In addition to water discharge, the tributary supplies substantial quantities of coarse sediment to the lower Spöl River and represents the primary source of sediment input downstream of the dams (Consoli et al., 2022; Scheurer & Molinari, 2003). Owing to the high sediment load supplied by the Ova da Cluozza, the river reach downstream of the confluence is substantially enriched in sediments and exhibits and active gravel bed morphology (Consoli et al., 2022). From the confluence, the Spöl River flows approximately 2.5 km before joining the Inn River near the village of Zernez. The present study focuses on a 1.5-km partially regulated reach immediately downstream of the Ova da Cluozza confluence (Figure 1), where the interaction between sediment supplied by the unregulated tributary and controlled flood releases from the Ova Spin Dam provides a unique setting for investigating geomorphic responses to sequential experimental floods.

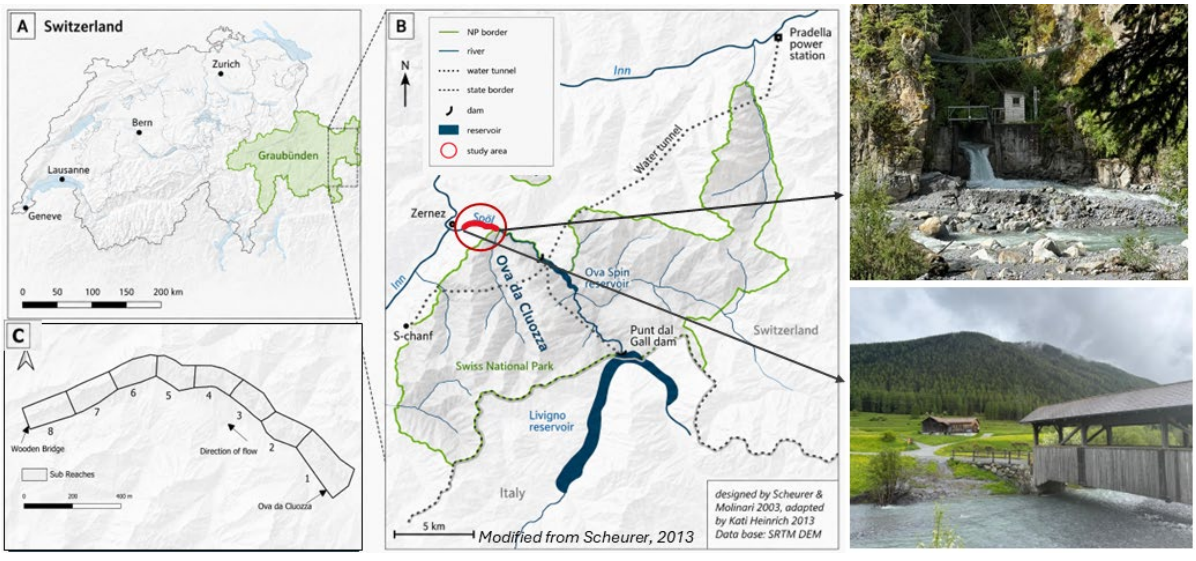


Figure 1: Location of the study area. (A) Location of the study area within the Canton of Graubünden, eastern Switzerland. (B) Overview of the lower Spöl River in the Swiss National Park showing the dams, the Ova da Cluozza tributary, the Inn River, the village of Zernez, the Swiss National Park boundary, and the study reach (red circle). (C) Schematic of the study reach showing the eight sub-reaches used for the spatial analyses. Photographs illustrate the upstream (Ova da Cluozza–Spöl confluence) and downstream (wooden bridge) limits of the study reach.

Between the pre-flood surveys conducted between 2018 and 2024, seven experimental floods were released from the Ova Spin Dam (Figure 2; Table A 1). Peak discharges ranged from 24.9 to 40.9 $m^3\ s^{-1}$, total flood durations from 8 to 19 h, and released volumes from 0.43 to 0.95 Mm^3, providing a diverse range of hydrological forcing conditions. The sequence comprised a single flood in 2018, two closely spaced floods in 2019, and individual releases in 2020, 2021, 2023, and 2024, while no experimental flood was released in 2022. Although most floods were released with comparable peak discharges (approximately 25 $m^3\ s^{-1}$), they differed substantially in hydrograph characteristics. The second flood in 2019 exhibited the highest peak discharge and released volume, the 2023 flood had the longest duration, and the 2024 flood was characterized by a double-

https://doi.org/10.5194/egusphere-2026-6858
Preprint. Discussion started: 12 November 2026
© Author(s) 2026. CC BY 4.0 License.

peaked hydrograph. Collectively, these controlled releases were designed to mobilize coarse sediment, redistribute gravel, maintain bar morphology, and enhance channel complexity, providing a unique opportunity to investigate cumulative geomorphic adjustment to repeated disturbances in a sediment-influenced regulated alpine river.

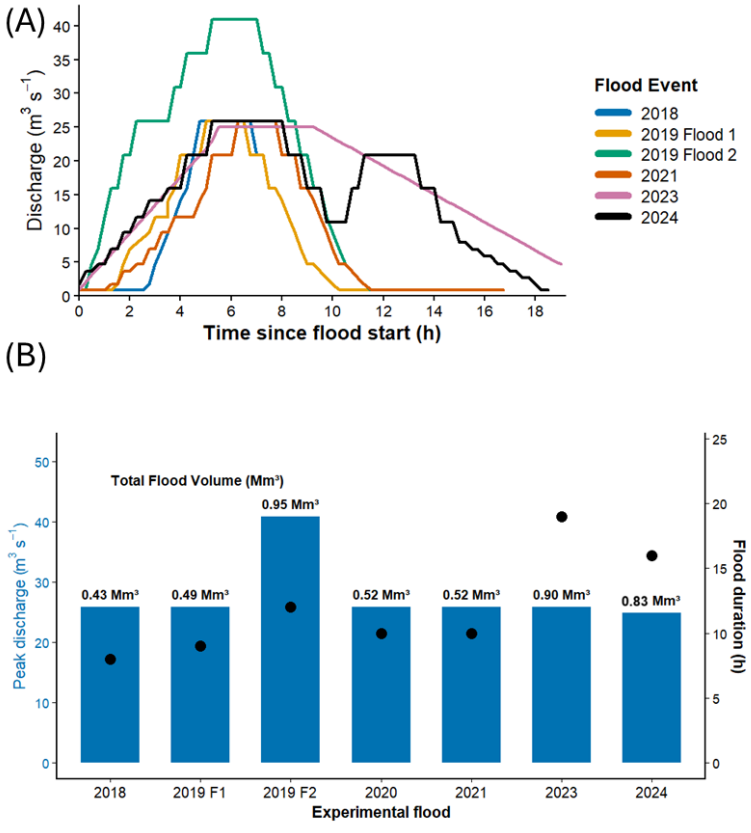


Figure 2: Location of the study area. (A) Location of the study area within the Canton of Graubünden, eastern Switzerland. Hydrological characteristics of the seven experimental floods released from the Ova Spin Dam between 2018 and 2024. Blue bars represent peak discharge (m³ s⁻¹), black points indicate total flood duration (h), and the values above the bars denote the total released flood volume (Mm³).

3 Materials and Methods

3.1 Field Data Collection

3.1.1 UAV Surveys and Photogrammetric Processing

This study combines high-resolution remote sensing and field observations to evaluate geomorphic responses of the lower Spöl River to experimental floods between 2018 and 2024. Experimental floods occurred in all study years except 2022, when no flood was released. Pre- and post-flood surveys were conducted for all flood events except the 2020 flood, when field campaigns could not be conducted due to COVID-19 restrictions.

https://doi.org/10.5194/egusphere-2026-6858
Preprint. Discussion started: 12 November 2026
© Author(s) 2026. CC BY 4.0 License.

Unmanned aerial vehicle (UAV) surveys equipped with RGB cameras were conducted by the SNP staff (except in 2018, survey that was performed by the Zurich University of Applied Sciences ZHAW) immediately before and after each flood event. The acquired imagery was processed using Structure-from-Motion (SfM) photogrammetry to generate sub-decimetric digital surface models (DSMs) and high-resolution orthomosaics of 0.1 m resolution. Representative orthomosaics from 2018, 2021, and 2024 are shown in Figure 3. Image processing, including DSM and orthomosaic generation, was performed using Pix4D software (Pix4D SA, n.d.). Details of the surveys, including survey dates, UAV platforms, and sensors used in each year, are provided in Table 1.

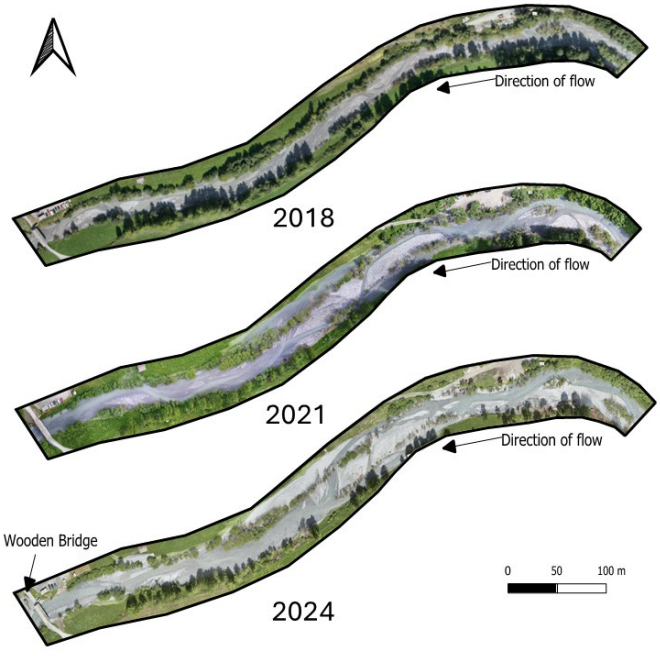


Figure 3: High-resolution orthophotos of the study reach for 2018, 2021, and 2024, illustrating temporal changes in channel morphology. The direction of flow is indicated, and key features such as the wooden bridge are marked for reference. The scale bar represents distance in meters.

Table 1: Details of UAV and sensor used for multi-year surveys

Experimental flood #	Data of Survey	UAV	Sensor
1	28.08.2018 and 11.09.2018	Wingtra One	RGB (Sony RX1; 42 MP)
2	18.06.2019 and 20.06.2019	Intel® Falcon 8	RGB (Sony NEX-7; 24.3 MP)
3	20.06.2019 and 25.06.2019	Intel® Falcon 8	RGB (Sony NEX-7; 24.3 MP)
4	21.06.2021 and 24.06.2021	DJI Matrice 210 RTK V2	RGB (Zenmuse X5S, 20.8 MP)
5	14.06.2023 and 16.06.2023	DJI Mavic 3E	RGB (4/3 CMOS, 20 MP)

https://doi.org/10.5194/egusphere-2026-6858
Preprint. Discussion started: 12 November 2026
© Author(s) 2026. CC BY 4.0 License.

6	10.06.2024 and 13.06.2024	DJI Matrice 350 RTK	RGB (Zenmuse P1, 45 MP)

3.1.2 Sediment Grain Size Surveys

Sediment grain size was measured at seven sites located on exposed gravel bars using the Wolman pebble count method (Wolman, 1954). Sediment particles were randomly selected, and the intermediate axis of each clast was measured using callipers. A minimum of 120 clasts were measured at each site to ensure representative sampling of grain-size distributions. Sampling was conducted before and after each experimental flood, except in 2020, when no field campaign was possible due to COVID-19 restrictions, and in 2022, when no flood occurred. In addition, grain-size data collected after the 2024 flood were lost due to unforeseen circumstances (Ruiz-Villanueva et al., 2026).

The collected grain-size data were processed to derive characteristic percentiles including D50 and D95. These initial-condition variables were subsequently explored in relation to geomorphic response indicators to assess their role in modulating flood-driven channel adjustment.

3.2 DSM Correction and Uncertainty Assessment

To ensure consistency between surveys, DSMs were corrected for potential orthorectification errors and inter-survey vertical misalignment (Jen & Chen, 2026; Peppa et al., 2019). Elevations were extracted from 50 stable reference points, including fixed infrastructure and large immobile boulders, distributed throughout the study reach. These reference points were used to quantify vertical offsets between surveys, and all DSMs were adjusted to a common elevation reference based on the identified shifts.

Spatially variable uncertainty associated with different land-cover types was addressed through a land-cover-specific multiple Level of Detection (LoD) approach (Neverman et al., 2016; Wheaton et al., 2010; Williams, 2012). Vector masks were manually delineated in QGIS using orthomosaics to identify exposed gravel surfaces, water surfaces and low land vegetation affected by reflectance, and shadowed regions (Dazzi, 2024). Separate LoD values were assigned to each class as the magnitude of uncertainty differs among each land cover type. Three alternative error sets were evaluated, and the final land-cover-specific uncertainty values (Table 2) were selected through sensitivity analysis based on comparison of the resulting DoDs with the orthomosaics to minimise spurious elevation changes while preserving geomorphically meaningful erosion and deposition patterns.

The selected land-cover-specific LoD values were incorporated into the Geomorphic Change Detection (GCD) software (Bailey, 2020). as spatially variable error surfaces. For each pixel, GCD combines the uncertainty values associated with the corresponding locations in the pre- and post-flood DEMs using a root-sum-of-squares propagation approach (Brasington et al., 2003; Wheaton et al., 2010). The propagated uncertainty defines the local minimum Level of Detection (LoD), against which the DoD elevation change is evaluated. Elevation changes whose absolute magnitude exceeds the propagated LoD are retained

https://doi.org/10.5194/egusphere-2026-6858
Preprint. Discussion started: 12 November 2026
© Author(s) 2026. CC BY 4.0 License.

as significant geomorphic change, whereas smaller changes are classified as indistinguishable from measurement uncertainty and excluded from further analysis.

Table 2: Land-cover-specific minimum Levels of Detection (LoD)

Land cover class	Error Set 1	Error Set 2	Error Set 3
	(m)	(m)	(m)
Water	0.3	0.2	0.2
Shadows	0.2	0.15	0.15
Gravel	0.1	0.05	0.05
Vegetation	0.1	0.1	0.2

The absence of bare-earth Digital Terrain Models (DTMs) posed an additional challenge due to the presence of vegetation within the study reach. Vegetation can introduce substantial uncertainty in photogrammetry-based surface differencing. To minimize vegetation-induced bias while maximizing the analysable area, regions containing vegetation in both pre- and post-flood DSMs were excluded from the analysis. Because channel widening and vegetation removal varied among years, the total active channel area analysed differed between survey periods (Figure A 1). Only elevation changes exceeding the corresponding local LoD thresholds were considered significant.

3.3 Geomorphic Change Detection

Topographic differencing (Lu et al., 2004) was performed at a spatial resolution of 0.1 m using Geomorphic Change Detection (GCD) standalone 7.5.0 software to generate Digital Models of Difference (DoDs) (Bailey, 2020).The resulting DoDs were used to quantify spatial patterns of erosion, deposition, and net sediment balance associated with each flood event in terms of both area and volume (Wheaton et al., 2010). Elevation changes were classified into minor, moderate, and strong erosion and deposition classes, whereas areas with changes below the minimum LoD are considered stable

To assess spatial variability in geomorphic response, the study reach was subdivided into eight sub-reaches numbered from upstream (SR1) to downstream (SR8), and geomorphic changes were analysed separately for each sub-reach following (Vericat and Batalla, 2006) before and after every flood event (Figure 1c).

The DoDs were used to calculate the area and volume of significant erosion and deposition, net sediment balance, and mean erosion and deposition depths for each flood. The depositional-to-erosional volume ratio was calculated as $V_{\mathrm{dep}}/V_{\mathrm{ero}}$, with values greater than 1 indicating deposition-dominated responses and values below 1 indicating erosion-dominated responses. Because the active channel area available for analysis differed among survey years owing to channel widening, vegetation removal and the exclusion of persistently vegetated areas, gross sediment mobilisation was normalised by the active area analysed for each event. This area-normalised metric, hereafter referred to as geomorphic activity, was calculated as:

https://doi.org/10.5194/egusphere-2026-6858
Preprint. Discussion started: 12 November 2026
© Author(s) 2026. CC BY 4.0 License.

$$\text{Geomorphic activity} = \frac{|V_{\text{ero}}| + V_{\text{dep}}}{A_{\text{active}}}, \quad (1)$$

where A_{active} is the total active channel area included in the corresponding DoD analysis. The metric has units of metres and represents the equivalent average depth of total sediment mobilisation across the analysed area. Unlike net volumetric change, it accounts for both erosion and deposition and therefore captures the overall magnitude of geomorphic activity even when the two components are approximately balanced.

3.4 Geomorphic Change Detection

Additional geomorphic analyses were conducted in QGIS to complement the topographic differencing results. These included the derivation of geomorphic indicators from the DSMs, such as surface roughness, used as a proxy for bed surface heterogeneity and calculated as the maximum absolute elevation difference between each raster cell and its eight neighbouring cells using the GDAL Roughness algorithm (GDAL/OGR contributors, 2024), and channel slope at both reach and sub-reach scales, together with analyses of channel width and cross-sectional adjustment.

Channel widths were mapped along transects drawn perpendicular to the channel centreline at 50 m intervals throughout the study reach under both pre- and post-flood releases. This approach enabled assessment of width adjustments associated with individual flood events as well as cumulative changes in channel width between 2018 and 2024. Flood-induced adjustments in channel width, surface roughness and slope were expressed as percentage changes between the corresponding pre- and post-flood median values.

$$\Delta X(\%) = \frac{X_{\text{post}} - X_{\text{pre}}}{X_{\text{pre}}} \times 100 \quad (2)$$

3.5 Flood Hydrograph Controls and Riverbed Initial Conditions

Flood hydrographs were characterized using six variables describing event magnitude, duration, and shape: peak discharge (Q_{peak}), peak-flow duration (T_{peak}), total released water volume (V_{total}), total flood duration (T_{total}), the ratio between rising- and falling-limb durations, and the number of hydrograph peaks (Table S 1). For the double-peaked 2024 event, peak-flow duration was calculated as the cumulative duration of both peak-flow periods, while the rising-to-falling-limb ratio was calculated at the event scale using the summed durations of the respective limb across the entire event.

Initial channel conditions were characterized by pre-flood surface grain size, channel slope, surface roughness, and the time elapsed since the most recent potentially morphologically effective event. Such events included previous experimental floods, natural floods originating from the Ova da Cluozza tributary, and operational dam releases, including flood-management and other extraordinary releases from Ova Spin Dam. Pre-flood median slope and median surface roughness were derived from the UAV-based DSM corresponding to each event. Surface roughness was calculated using the GDAL Roughness algorithm as the maximum absolute elevation difference between each raster cell and its eight neighbouring cells. Pre-flood D_{50}, derived from field-based pebble counts, was used to represent the initial sediment calibre where data were available.

https://doi.org/10.5194/egusphere-2026-6858
Preprint. Discussion started: 12 November 2026
© Author(s) 2026. CC BY 4.0 License.

Antecedent disturbance history was represented using two elapsed-time variables: time since the previous experimental flood (T_{exp}) described the sequence of scheduled experimental releases, whereas time since the last morphologically effective event (T_{LME}) also accounted for intervening flows capable of modifying channel morphology. Events with a discharge exceeding 10 $m^3 s^{-1}$ were classified as potentially morphologically effective. These included scheduled experimental floods, natural floods originating from the Ova da Cluozza, and non-experimental other dam flow releases from the dam for maintenance purposes. T_{LME} was calculated as the number of days between each experimental flood and the most recent preceding event exceeding this threshold.

The two elapsed-time metrics differed for the 2021, 2023 and 2024 floods because other potential morphologically active events such as either a natural flod from Cluozza or an operational dam releases occurred between consecutive experimental floods (Table 3). T_{LME} was therefore included to represent the interval since the most recent potentially morphology-altering flow, rather than only the interval between scheduled experimental floods.

The hydrograph variables and initial-condition indicators were subsequently evaluated as potential controls on the reach-scale geomorphic responses quantified from the pre- and post-flood surveys.

Table 3: Time since the previous experimental flood and time since the last potential morphologically effective event

Flood	Peak Discharge Q_{peak}	Peak Duration T_{peak}	Total Volume (m^3) V_{total}	Rising /falling duration ratio	Number of Peaks	Time since the last experimental flood (days)	Last Morphologically effective event	Event type	**Time since the most potential morphologically effective event (days)**
2018	25.9	2	430200	0.5	1	382	18.08.2017	2017's experimental flood	382
2019 F1	25.9	1.5	486360	0.75	1	288	04.09.2018	2018's experimental flood	288
2019 F2	40.9	1.75	950490	1.25	1	5	19.06.2019	2019's experimental flood #1	5
2021	25.9	1.5	515160	1.29	1	357	30.08.2020	Natural flood from the Ova da Cluozza	297
2023	25.9	4.5	904410	0.88	1	722	25.10.2022	Operational dam release	233
2024	24.9	4.75	835830	0.69	2	362	16.04.2024	Operational dam release	56

https://doi.org/10.5194/egusphere-2026-6858
Preprint. Discussion started: 12 November 2026
© Author(s) 2026. CC BY 4.0 License.

3.6 Statistical Analysis

The hydrograph characteristics and initial channel conditions described above were treated as potential predictors of flood-induced geomorphic response. To provide an integrated comparison of the six experimental floods, an event-fingerprint heatmap was constructed by ranking the floods separately within each predictor and response variable (Gŕaler et al., 2013). Ranks were rescaled between 0 and 1, where 0 represented the lowest observed value and 1 the highest. These ranks therefore represented the relative position of each flood within a given variable and did not indicate direct comparability among variables with different units.

Relationships between hydrograph characteristics, initial conditions and geomorphic responses were evaluated using Spearman's rank correlation coefficient (ρ). A predictor–response matrix was used to identify potential controls on geomorphic adjustment, while a separate response–response matrix was used to assess whether different components of channel response varied together. Correlations between pre-flood slope and percentage slope change, pre-flood roughness and percentage roughness change, and pre-flood D_{50} and percentage D_{50} change were not calculated because the initial value is mathematically embedded in its corresponding percentage-change metric.

Given the limited number of flood events, the correlation analysis was treated as exploratory. Sensitivity to individual floods was assessed using a leave-one-event-out procedure, in which each correlation was recalculated after sequentially omitting one flood. Directional robustness was expressed as the proportion of omission tests in which the correlation retained the same positive or negative direction as the correlation obtained from the complete dataset.

All statistical analyses and graphical synthesis were performed in R (R Core Team, 2025) using RStudio version 2025.05.1.

4 Results

4.1 Reach Scale Distribution of Erosion/ Deposition

The distribution of elevation change varied considerably among flood events, indicating substantial spatial heterogeneity in geomorphic response (Figure 4a). Except for the DoD maps, all figures present only elevation changes exceeding the minimum level of detection (LoD). In the DoD maps, areas with changes below the minimum LoD are shown as stable. Elevation differences generally ranged between −1 m and +1 m, with most changes concentrated between 0 and 0.5m, as reflected by interquartile ranges (Figure B 1). This suggests that most of the channel experienced relatively minor adjustments, while larger changes were confined to localized areas. The spatial patterns of geomorphic change associated with the six experimental floods are presented in the DoD maps (Figure 4), revealing substantial variability in the magnitude and spatial distribution of erosion and deposition among flood events. These maps provide the spatial framework for the reach- and sub-reach-scale analyses presented in the following sections.

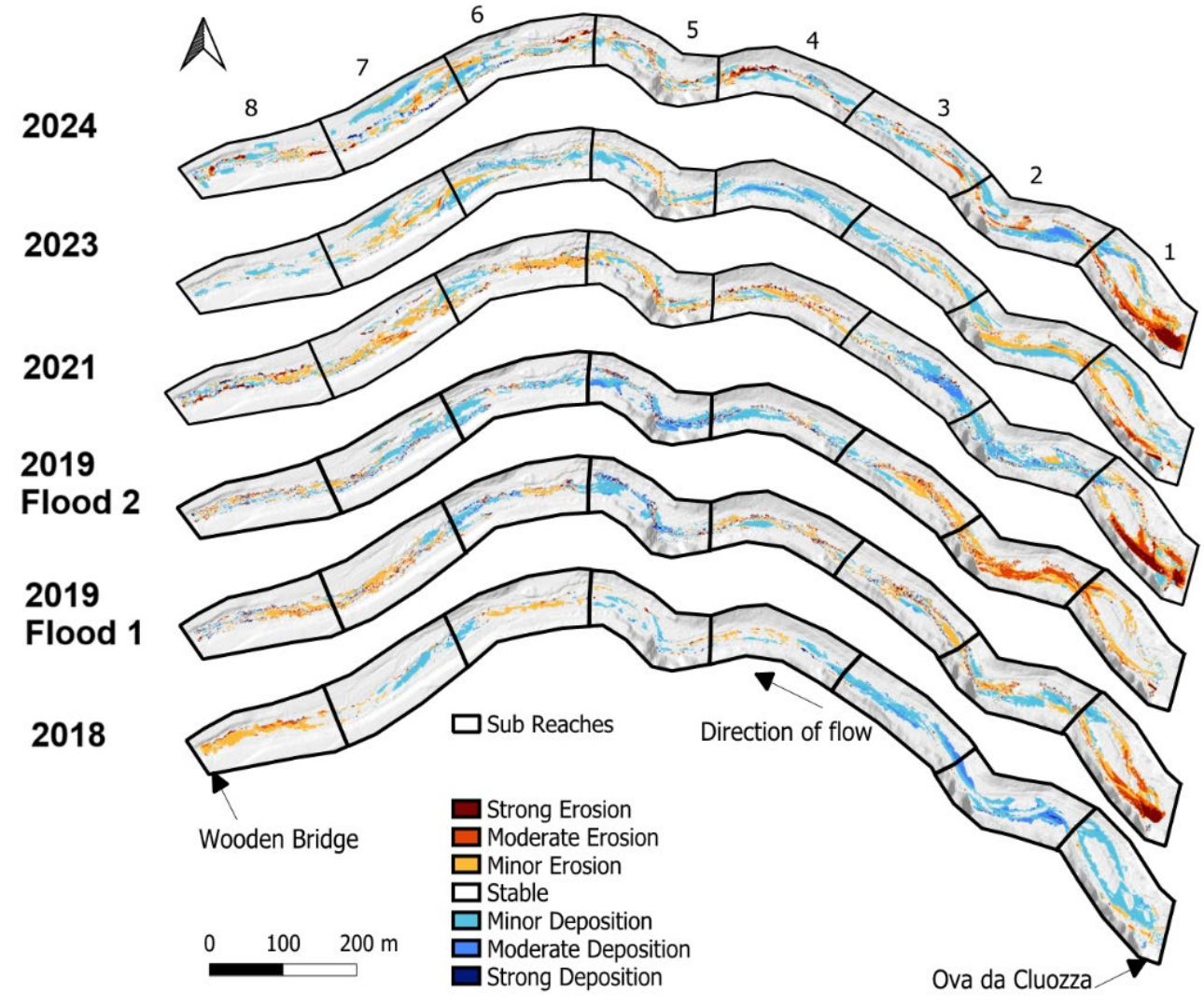
https://doi.org/10.5194/egusphere-2026-6858
Preprint. Discussion started: 12 November 2026
© Author(s) 2026. CC BY 4.0 License.

Event-wise histograms illustrating the spatial distribution of erosion and deposition are presented in Figure 5A. The 2018 and 2023 floods were predominantly depositional, with deposition affecting 74% and 61% of the active channel area, respectively. In contrast, erosion occupied a greater proportion of the channel during the 2019 Flood 1 (55%) and 2021 (57%) events, indicating a predominantly erosional response. The 2019 Flood 2 and 2024 floods exhibited nearly balanced spatial distributions, although erosion remained slightly dominant during the 2019 Flood 2 event (52%), whereas deposition occupied a marginally larger proportion of the channel during the 2024 flood (53%). Across all events, most elevation changes remained within ±0.5 m. The 2024 flood, however, displayed localized elevation losses exceeding the average depths, indicating the occurrence of deep but spatially restricted incision.

Volumetric analysis (Figure 5B) reveals differences in the magnitude of geomorphic change. Net deposition occurred during the 2018 (+2404 m^3) and 2023 (+483 m^3) floods, whereas the 2019 Flood 1 (−1301 m^3), 2019 Flood 2 (−319 m^3), 2021 (−2152 m^3), and 2024 (−2966 m^3) floods all resulted in net erosion. The contrast between spatial extent and volumetric change is particularly evident for the 2024 flood. Although deposition occupied a slightly larger proportion of the channel area, erosion volumes exceeded deposition volumes, indicating that erosion was concentrated in relatively small areas but occurred at substantially greater depths.

Mean depths of geomorphic change further support this pattern. Average erosion depths exceeded average deposition depths for most flood events, with the greatest erosion depth observed during the 2024 flood (0.71 m) and the lowest during the 2023 flood (0.36 m). Deposition depths were generally smaller, except for the 2021 event, which exhibited the highest mean deposition depth (0.54 m).

https://doi.org/10.5194/egusphere-2026-6858
Preprint. Discussion started: 12 November 2026
© Author(s) 2026. CC BY 4.0 License.



335 **Figure 4: Digital elevation models of difference (DoDs) illustrating the spatial patterns of erosion and deposition following the six experimental floods released between 2018 and 2024. Erosion is shown in red/orange colours and deposition in blue colour, each classified into minor, moderate, and strong intensity classes. The maps are displayed over the hillshade derived from the most recent DEM of 2025. The study reach is divided into eight sub-reaches (1–8) to facilitate the subsequent sub-reach-scale analyses.**

https://doi.org/10.5194/egusphere-2026-6858
Preprint. Discussion started: 12 November 2026
© Author(s) 2026. CC BY 4.0 License.

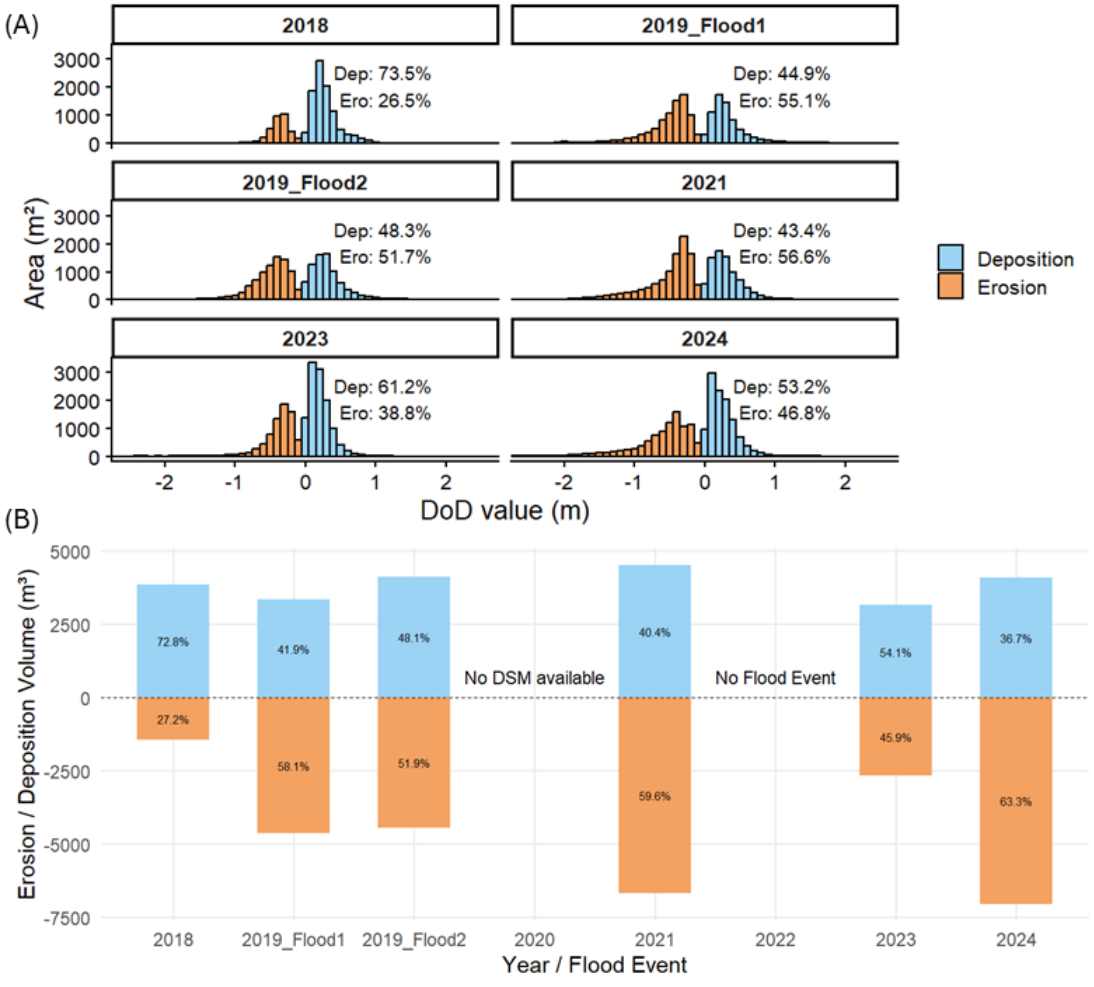


Figure 5: (A)Boxplots showing distribution of elevation change across different flood events. Blue Jittered points represent Deposition and Orange jittered points represent Erosion (B) Distribution of area affected by erosion and deposition across flood events from 2018 till 2024. Dep. And Ero. show the percentages of area that experienced Erosion or Deposition

4.2 Sub- Reach Scale Distribution of Erosion/ Deposition

The DoD maps (Figure 4) illustrate the spatial distribution of erosion and deposition within each sub-reach, while the heatmap (Figure 7) summarizes the corresponding net volumetric changes. The longitudinal distribution of net volumetric change varied

https://doi.org/10.5194/egusphere-2026-6858
Preprint. Discussion started: 12 November 2026
© Author(s) 2026. CC BY 4.0 License.

substantially among sub-reaches and flood events, highlighting considerable spatial heterogeneity in geomorphic response to the experimental floods.

The upstream sub-reach (SR1) consistently exhibited the largest negative volumetric changes across most flood events. Strong erosion was observed during several floods, including 2019 Flood 1 (−1708 m³), 2021 (−2160 m³), and 2024 (−2193 m³), indicating substantial sediment mobilization in the upstream portion of the study reach.

In contrast, the middle section of the reach (SR2–SR5) frequently exhibited net deposition. During the 2018 flood, strong deposition occurred in SR2 and SR3. Similarly, the 2019 Flood 2 event produced pronounced deposition in SR4 and SR5, with SR5 reaching approximately +1074 m³. The 2021 flood also resulted in substantial deposition in the middle reaches, particularly in SR2 (+980 m³) and SR3 (+788 m³).

The downstream section of the reach (SR6–SR8) showed more variable behaviour across experimental flood events. These sub-reaches experienced alternating phases of erosion and deposition, with some floods showing moderate erosion and others exhibiting localized deposition.

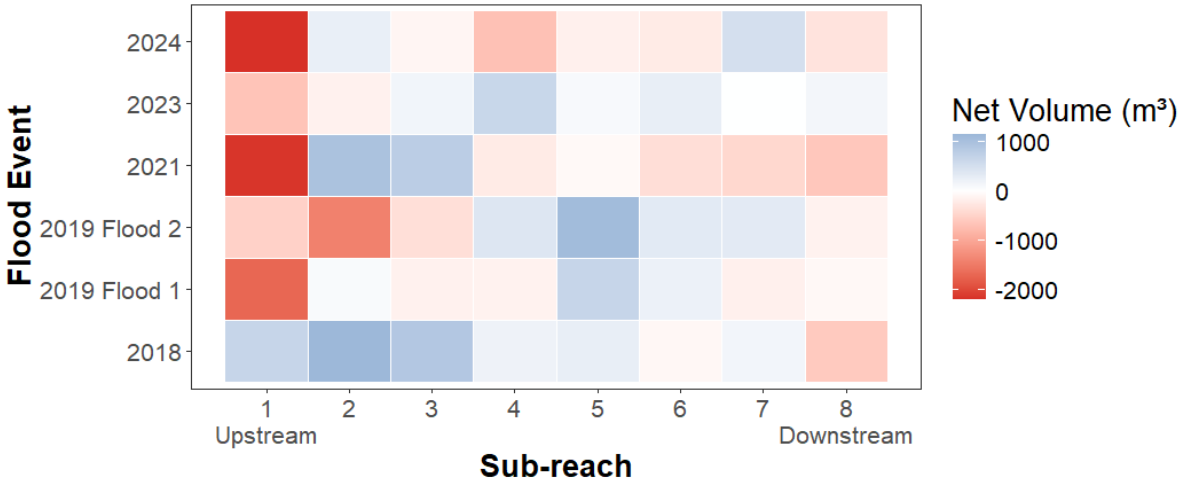


Figure 6: Net volumetric change across sub-reaches (SR1–SR8), where red indicates net erosion and blue indicates net deposition. The darkness of the color represents a higher value

Differences between flood events were also evident in the spatial distribution of geomorphic change. The 2018 flood was largely depositional across most sub-reaches, whereas the two floods in 2019 produced stronger upstream erosion accompanied by deposition in downstream reaches. The 2021 flood generated widespread sediment mobilization, particularly in the

https://doi.org/10.5194/egusphere-2026-6858
Preprint. Discussion started: 12 November 2026
© Author(s) 2026. CC BY 4.0 License.

upstream reach. In contrast, the 2023 flood exhibited relatively small volumetric changes across the reach, while the 2024 flood again produced strong upstream erosion.

4.3 Surface Roughness, Slope & Grain Size changes

The spatial distribution of surface roughness changes is presented in Figure 7, while pre- and post-flood roughness at the reach and sub-reach scales is summarised in Figure 8. Across all surveys, median reach-scale surface roughness ranged from approximately 0.013 to 0.078, whereas channel slope ranged from approximately 3° to 15°. Surface roughness and channel slope showed similar spatial patterns along the study reach, with relatively high values generally occurring in the middle sub-reaches and lower values toward the downstream sections (Figure B 2).

The roughness-difference maps revealed localized patches of both roughening and smoothing throughout the active channel, although their extent and magnitude varied among flood events (Figure 7). The 2018 flood produced a modest increase in reach-scale roughness and variability, with roughness increasing across most sub-reaches while maintaining an overall downstream-decreasing pattern (Figure 8). Following 2019 Flood 1, reach-scale roughness changed little despite a slight increase in variability, whereas sub-reach responses were spatially heterogeneous, with increases in SR5 and SR8 and decreases in SR3 and SR4. In contrast, 2019 Flood 2 produced a slight reduction in reach-scale roughness and variability, accompanied by localized increases in the upstream sub-reaches and reductions across several middle sub-reaches. The 2021 and 2023 floods resulted in only minor reach-scale changes, although localized increases and decreases remained evident at the sub-reach scale. In contrast, the 2024 flood produced the largest response of the study period, with a marked reduction in reach-scale roughness and widespread smoothing across the middle reaches (SR2–SR5).

https://doi.org/10.5194/egusphere-2026-6858
Preprint. Discussion started: 12 November 2026
© Author(s) 2026. CC BY 4.0 License.

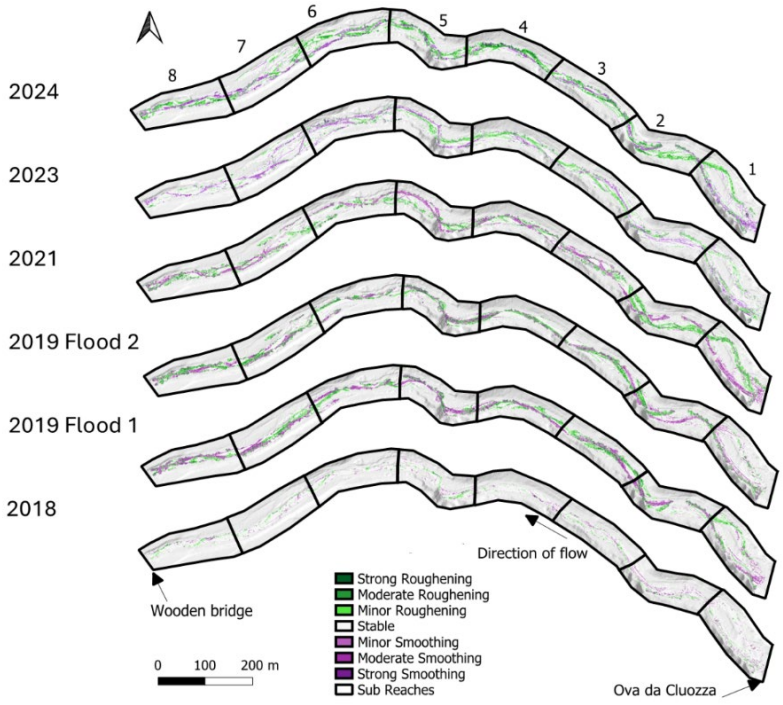


Figure 7: Spatial distribution of surface roughening and smoothing from 2018 to 2024. Green colours indicate increases in surface roughness (roughening) and purple colours indicate decreases in surface roughness (smoothing). Sub-reach boundaries (SR1–SR8) are shown to facilitate longitudinal comparison. The maps are displayed over a hillshade derived from the 2025 digital elevation model (DEM).

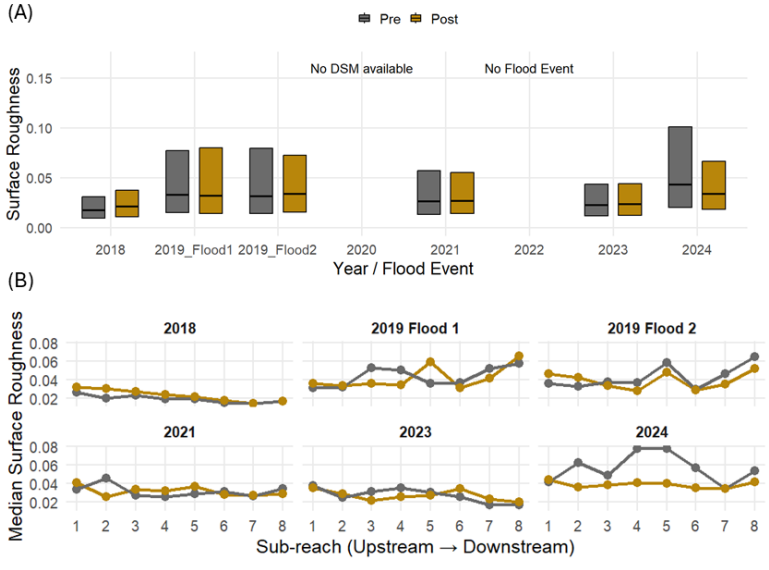


Figure 8: Surface roughness response to flood events at reach and sub-reach scales from 2018 to 2024. (a) Distribution of reach-scale surface roughness before (Pre) and after (Post) each flood event. (b) Median surface roughness at the sub-reach scale (SR1–SR8, upstream to downstream) before and after each flood.

https://doi.org/10.5194/egusphere-2026-6858
Preprint. Discussion started: 12 November 2026
© Author(s) 2026. CC BY 4.0 License.

Changes in sediment grain-size percentiles before and after the experimental floods are presented in Figure 9. Median grain size (D_{50}) increased from 21.5 to 27.0 mm following 2019 Flood 1, decreased slightly to 25.8 mm after Flood 2, declined from 24.2 to 23.2 mm following the 2021 flood, and increased markedly from 29.0 to 37.5 mm after the 2023 flood (Figure 9a). The D_{84} percentile increased from 41.0 to 46.0 mm following Flood 1, decreased to 43.5 mm after Flood 2, increased from 42.9 to 52.9 mm following the 2021 flood, and increased further from 60.0 to 65.0 mm after the 2023 flood (Figure 9b). The D_{95} percentile decreased slightly from 65.0 to 62.0 mm following Flood 1, increased to 65.0 mm after Flood 2, and increased substantially following the 2021 (61.7–96.1 mm) and 2023 (95.0–103.0 mm) floods (Figure 9c).

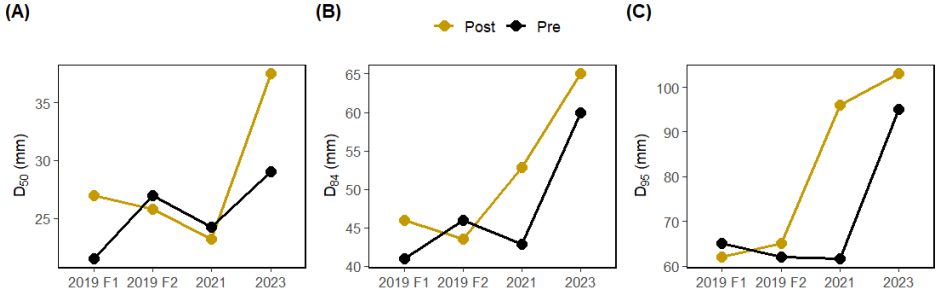


Figure 9: Comparison of surface sediment grain-size percentiles measured before (Pre) and after (Post) the experimental flood events. Panels show changes in (A) D_{50}, (B) D_{84}, and (C) D_{95} for the 2019 Flood 1 (F1), 2019 Flood 2 (F2), 2021, and 2023 flood events.

4.4 Changes in Channel Width

Comparison of pre- and post-flood conditions indicates only modest channel widening following individual experimental floods (Figure B 3). Median reach-scale width increased by less than 1.2% during the 2018–2021 floods, with slightly larger responses during the 2023 (3.69%) and 2024 (2.78%) floods, corresponding to absolute increases of approximately 1.2 m and 1.0 m, respectively.

At the sub-reach scale, widening was spatially heterogeneous and varied among flood events (Figure B 3). Localized widening shifted between upstream, mid-reach, and downstream sections, with the largest individual responses occurring in SR7 during the 2021 flood (5.46%) and in SR3–SR8 during the 2023 and 2024 floods. However, no persistent spatial pattern of widening was evident across successive floods.

4.5 Relationship of Flood Hydrological Characteristics with the Geomorphic Response of the River

The relationships between total flood volume and the reach-scale geomorphic response metrics is presented in Figure 10. Overall, total flood volume showed no consistent relationship with erosion volume, deposition volume, sediment mobilisation per active area or the deposition-to-erosion balance ratios. Among the response variables, channel widening showed the clearest positive association with total flood volume, although this relationship was not monotonic. Erosion volume varied considerably among events and did not increase systematically with total flood volume (Figure 10a). The 2021 and 2024 floods produced the largest erosion volumes, despite having lower total volumes than the 2019 Flood 2 and 2023 events. Conversely,

https://doi.org/10.5194/egusphere-2026-6858
Preprint. Discussion started: 12 November 2026
© Author(s) 2026. CC BY 4.0 License.

the high-volume 2023 event produced a comparatively low erosion volume. Deposition volume also varied among events without a clear relationship with total flood volume, with broadly comparable deposition volumes occurring across floods of different sizes (Figure 10b).

Sediment mobilisation per active area ranged from approximately 0.30 to 0.58 m (Figure 10e). The highest value occurred during the 2021 flood (0.58 m), whereas the 2023 flood produced the lowest value (0.30 m), despite having one of the largest total volumes and the longest total duration. The 2018, 2019 Flood 1, 2019 Flood 2 and 2024 events produced values of approximately 0.39, 0.50, 0.51 and 0.52 m, respectively. Total flood duration, represented by marker size in Figure 10e, therefore showed no uniform correspondence with sediment mobilisation per active area.

The volume- and area-based deposition-to-erosion ratios also varied independently of total flood volume (Figure 10c–d). The 2018 flood was strongly deposition-dominated, with volume- and area-based ratios of 2.70 and 2.81, respectively. The 2019 Flood 1, 2019 Flood 2 and 2021 events were erosion-dominated, with both ratios below unity. The 2023 event was deposition-dominated, with ratios of 1.18 by volume and 1.58 by area. In contrast, the 2024 event had a volume-based ratio of 0.58 and an area-based ratio of 1.05. Thus, erosion exceeded deposition by volume, although the spatial extents of erosion and deposition were approximately balanced.

Median channel width increased during all six floods, but the magnitude of widening differed among events (Figure 10f). Width increased by less than 1% during the 2018, 2019 Flood 1 and 2021 events, compared with 1.14% during 2019 Flood 2, 3.69% during 2023 and 2.78% during 2024. Although widening generally increased with total flood volume, the highest-volume event, 2019 Flood 2, produced substantially less widening than the slightly lower-volume 2023 event. The two events with the longest total durations, 2023 and 2024, also exhibited the greatest widening.

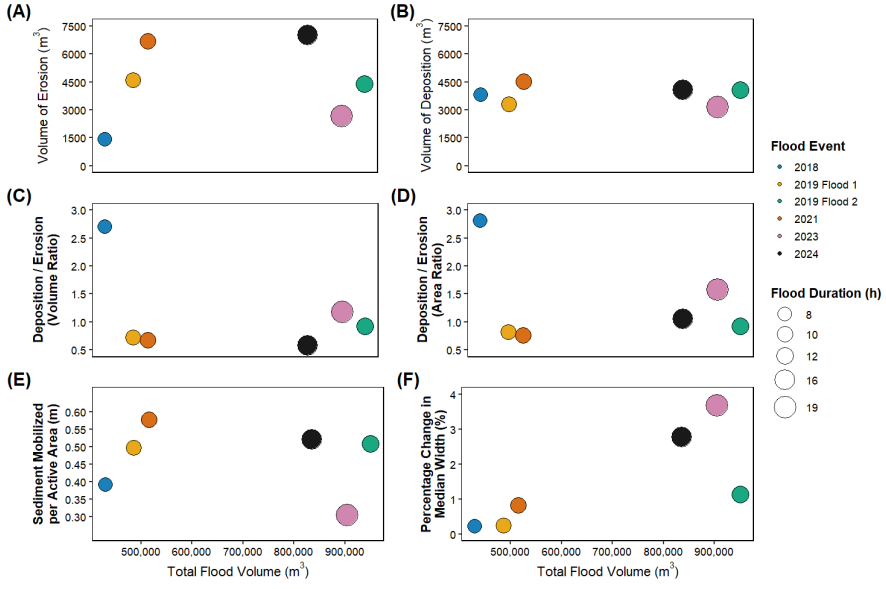


Figure 10: Relationships between total flood volume and geomorphic responses expressed as: (a) erosion volume, (b) deposition volume, (c) volume-based deposition-to-erosion ratio, (d) area-based deposition-to-erosion ratio, (e) sediment mobilisation per active

https://doi.org/10.5194/egusphere-2026-6858
Preprint. Discussion started: 12 November 2026
© Author(s) 2026. CC BY 4.0 License.

area and (f) percentage change in median channel width. Marker size represents total flood duration in all panels, and colours identify individual flood events.

Figure 11 presents the relationships between peak discharge, hydrograph asymmetry and selected geomorphic response metrics. Peak discharge showed no consistent relationship with sediment mobilisation per active area (Figure 11a). Five events had similar peak discharges of approximately 25–26 $m^3 s^{-1}$, but their sediment mobilisation values ranged from approximately 0.30 to 0.58 m. The 2019 Flood 2 event had the highest peak discharge, approximately 40.9 $m^3 s^{-1}$, but produced an intermediate sediment mobilisation value of approximately 0.51 m. Peak-flow duration also showed no consistent correspondence with sediment mobilisation. The 2023 and 2024 floods had the longest peak durations but produced contrasting mobilisation values of approximately 0.30 and 0.52 m, respectively. Events with shorter peak durations similarly produced a broad range of responses.

Hydrograph asymmetry, expressed as the ratio between rising- and falling-limb durations, showed no consistent relationship with sediment mobilisation or the deposition-to-erosion ratios (Figure 11b–d). Events with comparable asymmetry ratios produced different mobilisation and sediment-balance responses. The 2018 event had the highest volume- and area-based D/E ratios, whereas the 2019–2021 events generally remained below unity. The 2023 event was deposition-dominated by both measures, while the 2024 event was erosion-dominated by volume and approximately balanced by area.

The 2024 flood was the only event containing two peaks. It produced a sediment mobilisation value of approximately 0.52 m, a volume-based D/E ratio of 0.58 and an area-based ratio of 1.05. Because only one event contained two peaks, the dataset did not provide an event-to-event comparison of responses to single- and multiple-peak hydrographs.

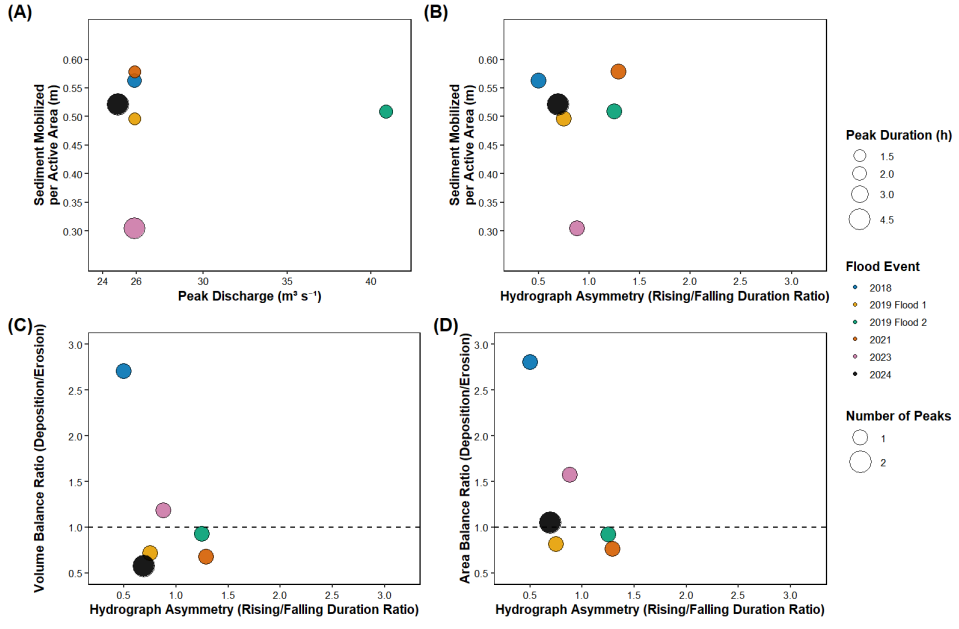


Figure 11: Relationship between flood hydrograph shape and geomorphic response across study events. (a) Rising-to-falling limb duration ratio versus sediment mobilized per unit area, (b) rising-to-falling limb duration ratio versus sediment mobilized per unit area (c) rising-to-falling limb duration ratio versus deposition-to-erosion ratio (volume), and (d) rising-to-falling limb duration ratio

https://doi.org/10.5194/egusphere-2026-6858
Preprint. Discussion started: 12 November 2026
© Author(s) 2026. CC BY 4.0 License.

versus deposition-to-erosion ratio (area).Colors distinguish individual floods. Dashed horizontal lines in (b) and (c) mark the threshold of unity, separating net depositional (>1) from net erosional (<1) conditions

Among the four floods with paired pre- and post-flood grain-size measurements, surface grain-size change showed no consistent correspondence with peak discharge or total flood volume. The 2019 Flood 2 event had the highest peak discharge and total volume but did not produce the greatest surface coarsening, whereas the 2023 event exhibited the largest increases in the reported grain-size percentiles.

4.6 Influence of pre-flood channel conditions on geomorphic response

4.6.1 Grain Size Distribution

The relationship between pre-flood median grain size (D_{50}) and sediment mobilization per active area is shown in Figure 13A. Grain-size data were available for four flood events and showed substantial variability in antecedent bed-surface conditions. Sediment mobilization generally decreased with increasing pre-flood D_{50}. The 2023 flood was associated with the coarsest bed surface (D_{50} = 29 mm) and the lowest sediment mobilization (0.304 m), whereas the 2021 flood exhibited the highest sediment mobilization (0.578 m) under intermediate grain-size conditions (D_{50} = 24.2 mm). The two flood releases in 2019 showed comparable sediment mobilization despite different pre-flood D_{50} values (21.5 and 27.0 mm). Similar patterns were observed for the coarser grain-size fractions (D_{84} and D_{95}; Figure C 1). Comparable patterns were also observed for the coarser grain-size fractions (D_{84} and D_{95}; Figure C 1), with the 2023 flood exhibiting the coarsest bed-surface conditions and the lowest sediment mobilization, whereas the 2021 flood showed the highest sediment mobilization under intermediate D_{84} and D_{95} values.

4.6.2 Channel Slope and Roughness

The relationships between pre-flood median channel slope, pre-flood median surface roughness, and sediment mobilization per active area are shown in Figure 13C and D. Pre-flood median channel slope ranged from 4.22° in 2018 to 10.35° in 2024 (Figure 13C). The highest sediment mobilization was observed for the 2021 flood under an intermediate pre-flood slope (6.60°), whereas the lowest sediment mobilization occurred during the 2023 flood at a lower slope (5.63°). The two flood releases in 2019 exhibited similar pre-flood slopes (8.15° and 8.21°) and comparable sediment mobilization, while the 2024 flood was characterized by the steepest pre-flood slope and an intermediate sediment mobilization value.

Pre-flood median surface roughness varied from 0.019 in 2018 to 0.052 in 2024 (Figure 13D). The highest sediment mobilization occurred during the 2021 flood at an intermediate roughness value (0.031), whereas the lowest sediment mobilization was recorded for the 2023 flood (0.026). The two flood releases in 2019 exhibited similar pre-flood roughness values (0.039–0.040) and comparable sediment mobilization, while the highest roughness measured in 2024 corresponded to an intermediate sediment mobilization value.

https://doi.org/10.5194/egusphere-2026-6858
Preprint. Discussion started: 12 November 2026
© Author(s) 2026. CC BY 4.0 License.

4.6.3 Time since the last experimental flood (T_{EXP})

The relationship between the time elapsed since the previous flood and sediment mobilization per active area is shown in Figure 13B. The inter-flood interval ranged from 5 days before the second 2019 flood to 722 days before the 2023 flood. The highest sediment mobilization was observed during the 2021 flood after an interval of 357 days, whereas the lowest sediment mobilization occurred during the 2023 with the longest inter-flood period. The two flood events in 2019 were separated by 5 days and 288 days, respectively, and exhibited comparable sediment mobilization. The 2018 and 2024 floods occurred after intervals of 382 and 362 days, respectively, and were associated with intermediate sediment mobilization value

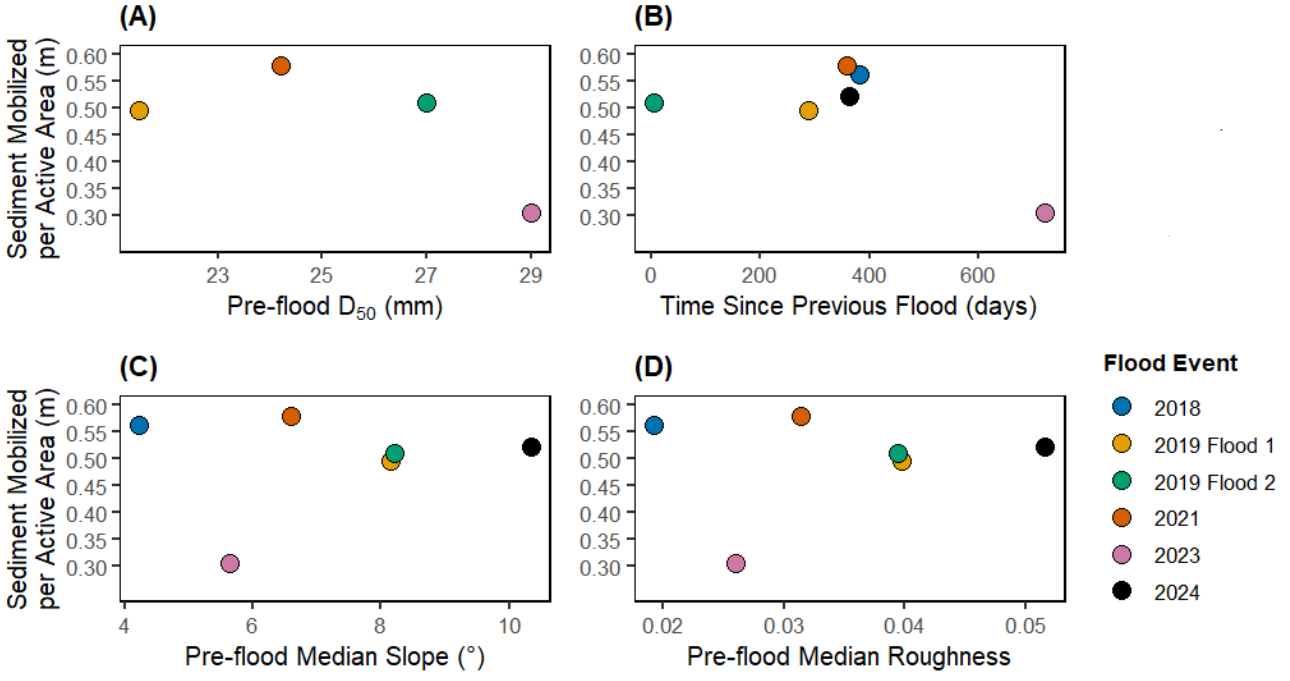


Figure 12: Relationships between sediment mobilized per active area and initial channel conditions. (A) Pre-flood median grain size (D_{50}), (B) time since the last experimental flood, (C) pre-flood median channel slope, and (D) pre-flood median surface roughness.

4.6.4 Time since the last morphologically effective event (T_{LME})

Time since the last morphologically effective event (T_{LME}) ranged from 5 days before the second 2019 flood to 382 days before the 2018 flood. Sediment mobilisation showed no consistent variation with T_{LME}: the highest value occurred during the 2021 flood after 297 days, whereas the lowest occurred during the 2023 flood after 233 days. The two 2019 floods followed intervals of 288 and 5 days but produced comparable levels of mobilisation, while the 2024 flood generated relatively high mobilisation after only 56 days. The 2018 flood, which followed the longest interval, exhibited the highest D/E volume ratio (2.704),

https://doi.org/10.5194/egusphere-2026-6858
Preprint. Discussion started: 12 November 2026
© Author(s) 2026. CC BY 4.0 License.

whereas the 2024 flood showed the lowest ratio (0.580). However, the remaining events did not display a consistent change in sediment balance with increasing T_{LME}.

4.7 Integrated Reach Scale Synthesis

The event-fingerprint heatmap revealed distinct combinations of hydrograph characteristics, initial channel conditions and geomorphic responses among the six floods, with no event consistently ranking highest across all variable groups (Figure 13A). The 2018 flood combined relatively low hydrograph magnitude and low pre-flood slope and roughness with the longest T_{LME}. It exhibited the highest D/E ratio and the largest positive changes in slope and roughness, but relatively low sediment mobilisation and channel widening. The first 2019 flood had relatively low flood volume and duration and produced limited channel widening, moderate sediment mobilisation and a marked increase in D_{50}. The second 2019 flood had the highest peak discharge and total flood volume, but its sediment mobilisation and channel-width response remained intermediate relative to the other events. The 2021 flood produced the highest sediment mobilisation and mean deposition depth, despite intermediate hydrograph characteristics. In contrast, the 2023 flood had the longest total duration and produced the greatest channel widening and increase in D_{50}, while recording the lowest sediment mobilisation. The 2024 flood was characterised by the longest peak duration, two discharge peaks and the steepest and roughest pre-flood channel. It also exhibited the greatest mean erosion depth, the lowest D/E ratio and the largest reductions in slope and roughness.

The predictor–response matrix identified several strong reach-scale associations (Figure 13B). Among the hydrograph characteristics, total flood duration was perfectly positively correlated with channel-width change ($\rho = 1.00$), while total flood volume was also strongly positively correlated with width change ($\rho = 0.83$). Peak duration was strongly negatively correlated with mean deposition depth ($\rho = -0.84$), whereas hydrograph asymmetry was positively correlated with deposition depth ($\rho = 0.60$). Pre-flood slope and roughness showed negative correlations with the D/E ratio ($\rho = -0.77$ and -0.83, respectively) and positive correlations with mean erosion depth ($\rho = 0.71$ and 0.77, respectively). T_{LME} was negatively correlated with channel-width change ($\rho = -0.71$) and positively correlated with changes in slope and roughness ($\rho = 0.60$ for both). For the four floods with complete grain-size data, pre-flood D_{50} was positively correlated with channel-width change ($\rho = 1.00$) and the D/E ratio ($\rho = 0.80, n = 4$). The strongest associations retained their direction in all leave-one-event-out iterations. Correlations between each pre-flood condition and its corresponding percentage-change metric were excluded because of structural coupling.

https://doi.org/10.5194/egusphere-2026-6858
Preprint. Discussion started: 12 November 2026
© Author(s) 2026. CC BY 4.0 License.

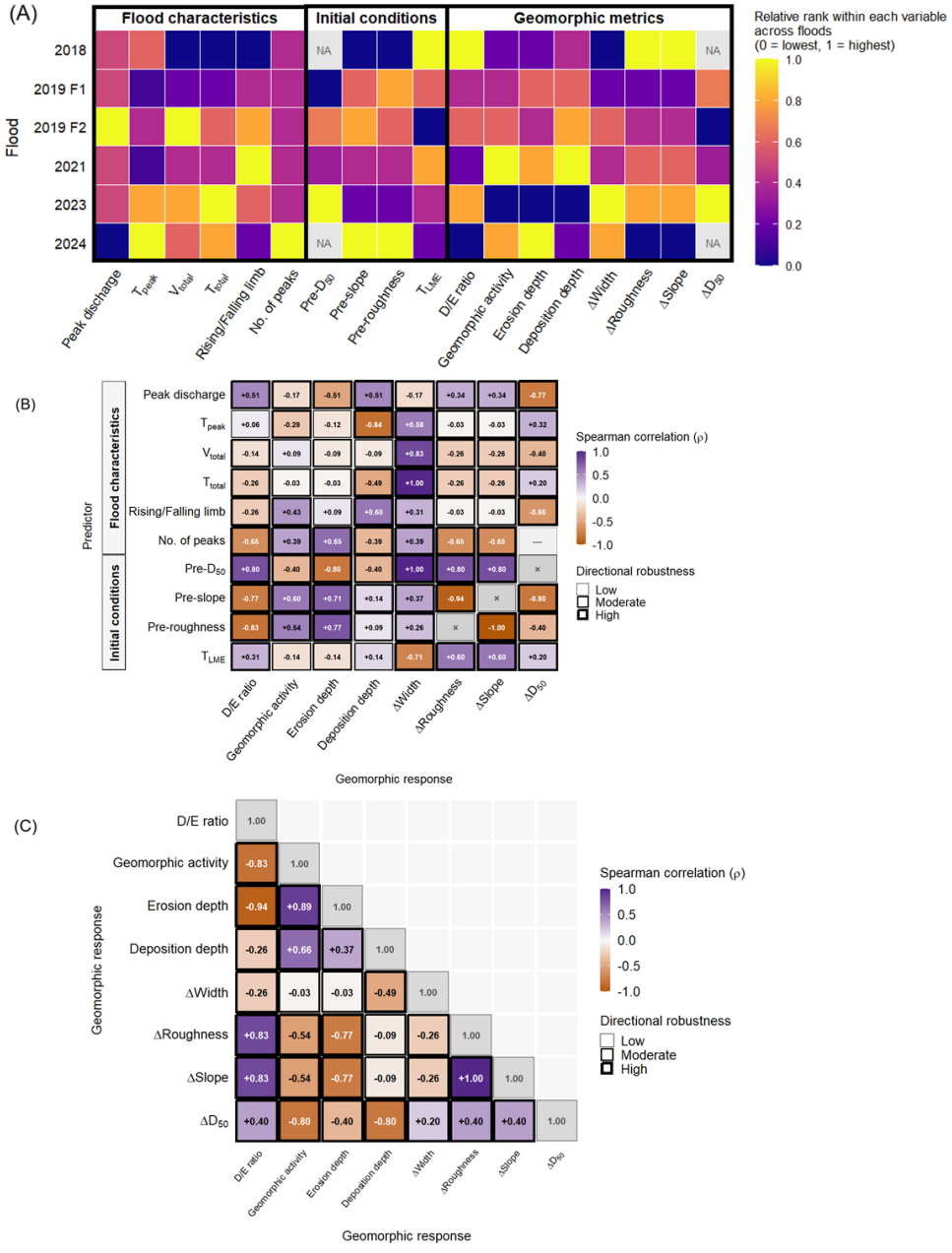


Figure 13: Integrated reach-scale synthesis of the six experimental floods. (A) Relative event ranks across hydrograph characteristics, initial conditions and geomorphic responses. (B) Spearman correlations between predictors and responses. (C) Correlations among response metrics. Tile colour indicates ρ, border thickness indicates directional robustness, crosses mark excluded structurally coupled relationships and dashes indicate undefined correlations. Relationships involving D50 are based on four events; all others use six.

https://doi.org/10.5194/egusphere-2026-6858
Preprint. Discussion started: 12 November 2026
© Author(s) 2026. CC BY 4.0 License.

The response–response matrix showed strong covariation among several components of geomorphic adjustment (Figure 13C). Percentage changes in median slope and roughness were perfectly positively correlated ($\rho = 1.00$). Sediment mobilization per active area was strongly positively correlated with mean erosion depth ($\rho = 0.89$) and negatively correlated with the D/E ratio ($\rho = -0.83$). Mean erosion depth was also strongly negatively correlated with the D/E ratio ($\rho = -0.94$) and with changes in slope and roughness ($\rho = -0.77$ for both). Conversely, the D/E ratio was positively correlated with changes in slope and roughness ($\rho = 0.83$ for both). Mean deposition depth showed a moderate positive correlation with sediment mobilization ($\rho = 0.66$.) For the four events with complete grain-size measurements, percentage change in $D_{50}$was negatively correlated with sediment mobilisation and mean deposition depth ($\rho = -0.80$ for both, $n = 4$). Channel-width change showed weak relationships with sediment mobilisation and mean erosion depth.

5 Discussion

5.1 Scope and Limitations of the Study

The interpretation of geomorphic change presented in this study should be considered within the context of several methodological and data-related limitations. Multi-temporal comparisons were derived from datasets acquired using different survey platforms, sensors, processing workflows, and operators, while terrain reconstruction relied on Structure-from-Motion (SfM) photogrammetry. These factors inevitably introduce uncertainties associated with image quality, reconstruction algorithms, software implementations, processing parameters, and the comparability of surface models (Eltner et al., 2016; James et al., 2019). Although these effects were minimised through careful co-registration, vertical alignment, consistent processing strategies where possible, and land-cover-specific uncertainty masking, residual uncertainties cannot be entirely eliminated, and the individual influence of these factors on reconstructed surface models was not evaluated explicitly (Eltner et al., 2016; Westoby et al., 2012).

Uncertainty associated with land-cover-specific errors represents an additional limitation. Approximate error values were assigned to different surface types (e.g., gravel bars, water, vegetation, and shadowed areas) for DoD analysis. Although sensitivity of multiple error scenarios was tested to select a representative threshold, spatial variability within individual land-cover classes may lead to localised deviations that are not fully captured by uniform error assumptions. This limitation is consistent with broader challenges in DoD-based analyses, where spatially variable uncertainty can influence the detection of geomorphic change (Wheaton et al., 2010).

The absence of bare-earth digital terrain models (DTMs) constitutes a further constraint. The use of digital surface models (DSMs) introduces potential artefacts from vegetation, particularly along channel banks. Despite masking procedures, areas with dense vegetation and large trees could not be reliably included, resulting in underrepresentation of geomorphic change in these zones. In particular, erosion or deposition processes along the banks may be underestimated due to limited visibility beneath vegetation cover.

https://doi.org/10.5194/egusphere-2026-6858
Preprint. Discussion started: 12 November 2026
© Author(s) 2026. CC BY 4.0 License.

Finally, a formal error propagation or probabilistic uncertainty analysis was beyond the scope of this study. Despite these limitations, the adopted workflow follows established best practices for SfM-based geomorphic change detection (James et al., 2019; Wheaton et al., 2010) and provides a robust basis for quantifying reach-scale patterns of erosion, deposition, channel widening, and associated morphological adjustments. The identified limitations therefore define the scope of the present study rather than diminish the reliability of the observed geomorphic patterns.

Beyond these methodological considerations, the temporal scope of the study also constrains the interpretation of the results. The analyses quantify geomorphic adjustments immediately before and after experimental flood releases and therefore capture the direct effects of individual floods. However, the processes governing sediment supply and availability between successive flood events were not investigated. These inter-flood processes are likely to influence antecedent channel conditions and, consequently, the geomorphic effectiveness of subsequent floods.

5.2 Drivers of geomorphic response: insights from the Spöl River

All six experimental floods were geomorphically effective, but their event fingerprints revealed substantial differences in the magnitude and form of channel adjustment. The 2018 and 2023 floods produced net depositional responses, consistent with previous observations of deposition following experimental releases in the Spöl River (Consoli et al., 2022; Hashemi et al., 2024; Pellegrini et al., 2022). In contrast, both 2019 floods, the 2021 event and particularly the 2024 flood were erosion dominated (Dazzi, 2024). These alternating responses indicate that successive floods did not act on equivalent channel states but inherited the morphological and sedimentary legacy of preceding events, as commonly observed in regulated gravel-bed rivers (Lisle & Church, 2002; Madej et al., 2009).

The integrated predictor–response analysis showed that hydrograph characteristics influenced specific components of channel adjustment rather than determining overall geomorphic effectiveness. Total flood duration and total flood volume were strongly associated with channel widening, while peak duration showed a weak relationship with mean geomorphic response metrics. In addition, the influence of peak discharge could not be assessed robustly because five of the six floods had very similar peak discharges, with only the second 2019 flood with a higher peak discharge. Longer or larger releases therefore appeared to favour lateral adjustment but did not consistently produce greater sediment mobilisation or a more erosion-dominated sediment balance. These results demonstrate that flood magnitude alone is insufficient to predict the geomorphic outcome of experimental releases (Gervasi et al., 2021; Magilligan et al., 2015; Phillips et al., 2018).

The contrasting responses of the two 2019 floods illustrate the influence of event sequencing. The second flood had the highest peak discharge and total flood volume yet produced only intermediate sediment mobilisation and channel widening. The five-day interval separating the two floods likely limited the amount of readily available material remaining for mobilisation. The first flood may have removed or redistributed accessible sediment and reorganised the bed surface, causing the second release to rework previously mobilised material rather than generate a proportionally larger response. Similar behaviour has been documented in regulated rivers, where closely spaced floods progressively reduce sediment availability or redistribute

https://doi.org/10.5194/egusphere-2026-6858
Preprint. Discussion started: 12 November 2026
© Author(s) 2026. CC BY 4.0 License.

sediment already stored within the channel (Hashemi et al., 2024; Madej et al., 2009; Schmidt and Grams, 2011; Schmidt and Wilcock, 2008).

The 2021 flood provides the clearest contrast to this magnitude-based expectation. Despite hydrograph characteristics comparable to several other events, it produced the highest area-normalised sediment mobilisation and the greatest mean deposition depth. This response suggests that substantial quantities of mobile sediment were available before the release. The Ova da Cluozza is the principal sediment source to the study reach, and tributary inputs between experimental floods may have replenished channel storage and increased the quantity of transportable material. Although the magnitude and timing of this sediment supply could not be quantified, the 2021 event indicates that sediment availability may exert a stronger control on geomorphic effectiveness than hydraulic forcing alone (Magilligan et al., 2015; Righini et al., 2017; Wolman and Miller, 1960).

The 2018 event similarly highlights the importance of initial conditions. It followed the longest interval since the last morphologically effective event and occurred under comparatively low pre-flood slope and roughness. Despite its relatively modest hydrograph, it exhibited the highest deposition-to-erosion ratio and the largest positive changes in slope and roughness. The long disturbance-free interval may have allowed sediment to accumulate within the reach, favouring redistribution and deposition during the subsequent release. However, the absence of a consistent relationship between T_{LME} and sediment balance across the remaining floods shows that elapsed time alone cannot represent sediment availability or channel preparedness. Thus, antecedent conditions should be evaluated using both the elapsed time and the geomorphic significance of previous events, rather than T_{LME} alone.

This is particularly evident for the 2023 flood. Although it had the longest total duration and one of the largest released volumes, it produced the lowest sediment mobilisation while generating the greatest channel widening and increase in D_{50}. Two maintenance releases from the Ova Spin dam in October 2022 (24 October: ~15 $m^3 s^{-1}$ for 3.25 h; 25 October: ~10 $m^3 s^{-1}$ for 2 h), approximately likely modified the bed before the 2023 experimental flood. These releases may have selectively removed finer particles and contributed to the observed pre-flood surface coarsening. A coarser and more stable surface would increase the threshold for sediment entrainment, thereby limiting bed mobilisation during the subsequent release (Church, 2006; Lisle and Church, 2002). The 2023 event therefore demonstrates why the time since the previous experimental flood alone is an incomplete descriptor of antecedent conditions; intervening releases capable of restructuring the bed must also be considered (Madej et al., 2009; Schmidt & Wilcock, 2008).

The comparison between areal and volumetric responses further emphasizes the spatial heterogeneity of geomorphic processes. Events such as 2024 demonstrate that deposition can dominate in terms of area while erosion dominates in terms of volume, indicating that erosional processes are more spatially concentrated but of greater magnitude. This interpretation is supported by consistently higher average erosion depths relative to deposition depths and aligns with observations of localized, high-intensity incision associated with experimental flood releases in the Spöl River. Such contrasts between the spatial extent and magnitude of geomorphic change highlight the importance of distinguishing between process intensity and spatial coverage (Wheaton et al., 2010).

https://doi.org/10.5194/egusphere-2026-6858
Preprint. Discussion started: 12 November 2026
© Author(s) 2026. CC BY 4.0 License.

Channel widening was strongly associated with total flood duration and total flood volume, suggesting that sustained hydraulic forcing favoured bank erosion and lateral adjustment. This is consistent with observations from natural and regulated gravel-bed rivers, where prolonged high flows promote channel expansion (Buraas et al., 2014; Gupta and Fox, 1974; Ruiz-Villanueva et al., 2023; Wolman and Miller, 1960). The experimental floods therefore continued to counteract channel narrowing in the Spöl, although widening during individual events remained modest relative to longer-term channel adjustment (Bertoldi et al., 2025; Hashemi et al., 2024).

Spatial patterns within the study reach provide additional insight into the controls on geomorphic adjustment. The persistent dominance of erosion within the upstream reach (SR1) indicates that this section functions as the principal sediment source during experimental floods, consistent with previous observations for the lower Spöl River (Consoli et al., 2022; Dazzi, 2024). In contrast, the middle reaches (SR2–SR5) predominantly act as zones of temporary sediment storage, where material eroded upstream is deposited and redistributed before subsequent remobilisation. Such spatial decoupling between sediment sources and sinks is characteristic of gravel-bed rivers, in which intermediate storage elements regulate downstream sediment transfer (Lisle and Church, 2002; Madej et al., 2009). The downstream reaches (SR6–SR8) exhibit more variable behaviour, reflecting a transitional role between sediment storage and transport, with alternating erosion and deposition indicating repeated sediment reworking rather than persistent accumulation.

Collectively, these findings demonstrate that geomorphic effectiveness cannot be explained by flood hydrograph characteristics alone. Although total flood volume emerged as a somewhat better, although not exclusive, predictor of sediment mobilization than peak discharge or flood duration, no single hydraulic metric consistently explained the observed geomorphic responses. Instead, flood response reflects the interaction between hydraulic forcing and antecedent channel conditions, including sediment availability, tributary sediment connectivity, bed surface condition, channel morphology, and the legacy of previous flood events. Consequently, geomorphic effectiveness should be viewed as an emergent property arising from the combined influence of flood characteristics and inherited channel conditions rather than from discharge magnitude alone (Magilligan et al., 2015; Righini et al., 2017; Wolman and Miller, 1960).

5.3 Interactions among geomorphic responses during channel adjustment

No single geomorphic metric adequately characterizes channel response because each quantifies a different aspect of adjustment. Sediment budgets describe the overall redistribution of sediment, erosion and deposition, depths represent the intensity of vertical reworking, channel widening reflects lateral adjustment, roughness and slope characterize bed morphology, and grain size indicates sediment sorting and armouring. Their combined interpretation therefore provides a more comprehensive understanding of flood-induced channel evolution than any individual metric.

The reach-scale synthesis showed strong coupling among sediment mobilisation, erosion depth and sediment balance. Greater mobilisation coincided with deeper erosion and lower D/E ratios, indicating that the most geomorphically active floods tended to be more erosion dominated (Church, 2006). Deposition depth was less strongly related to total mobilisation, suggesting that variation in overall activity was controlled primarily by erosion intensity rather than deposition alone.

https://doi.org/10.5194/egusphere-2026-6858
Preprint. Discussion started: 12 November 2026
© Author(s) 2026. CC BY 4.0 License.

Channel widening showed only weak reach-scale associations with sediment mobilisation and mean erosion depth, indicating that lateral adjustment was not directly proportional to vertical channel reworking (Buraas et al., 2014; Ruiz-Villanueva et al., 2023). This was particularly evident in 2023, when the greatest widening coincided with the lowest sediment mobilisation per active area, indicating that lateral adjustment and bed-level reworking did not vary consistently together. Although bank erosion can contribute to widening, the eroded material may be deposited locally, transferred downstream or combined with sediment supplied by the Ova da Cluozza. Channel-width change therefore reflects a distinct component of adjustment and should not be used as a direct proxy for total sediment mobilisation or sediment balance.

Surface grain-size change was also not directly proportional to geomorphic activity. For the four floods with complete observations, greater mobilisation and deposition depth were associated with relative reductions in D_{50}, rather than systematic coarsening. Highly active floods may therefore redistribute finer material across exposed surfaces, while coarsening depends on selective transport and armour development (Dietrich et al., 1989). The fining after the second 2019 flood may similarly reflect redistribution of finer sediment mobilised during the first event, although the limited number of complete observations requires cautious interpretation.

Changes in median slope and roughness were strongly coupled, indicating that channel-gradient adjustment and bed-surface structure evolved together (Church, 2006; Rickenmann and Recking, 2011). However, their relationships with the D/E ratio were weak, suggesting that sediment balance alone did not determine whether the channel became steeper, flatter, rougher or smoother. Deposition may increase slope and roughness through bar formation and uneven sediment accumulation, but it may also flatten and smooth the bed. Similarly, erosion may reduce topographic variability through bed lowering and reworking or increase it through incision, incision and exposure of coarse material. The direction of change therefore depended on the spatial organisation and intensity of geomorphic processes rather than simply on whether an event was erosion or deposition dominated.

The event sequence illustrates this variability. The 2018 flood increased both slope and roughness, whereas the two 2019 events and the 2023 flood produced comparatively limited changes. In contrast, the pronounced reductions during 2024 indicate widespread bed flattening and smoothing. Floods may therefore either enhance morphological heterogeneity through bar development and sediment organisation or reduce it through bedform reworking and sediment redistribution (Venditti et al., 2012). The magnitude of the 2024 response may also have been amplified by pre-flood protection works that altered the initial bed configuration and introduced redistributed sediment for subsequent reworking (Yager et al., 2012).

Overall, vertical reworking, lateral widening, sediment sorting and bed-surface restructuring were only partly coupled. Geomorphic effectiveness should therefore be evaluated using multiple complementary indicators that distinguish the magnitude, direction and morphological expression of channel adjustment.

5.4 Geomorphic effectiveness across temporal scales: Implications for environmental flow design

The experimental floods were clearly effective at the event scale, repeatedly mobilising sediment, promoting lateral adjustment and reworking the channel bed. However, comparison with the longer-term evolution of the lower Spöl reveals a marked scale

https://doi.org/10.5194/egusphere-2026-6858
Preprint. Discussion started: 12 November 2026
© Author(s) 2026. CC BY 4.0 License.

dependence in geomorphic effectiveness (Bertoldi et al., 2025; Sheikh et al., in press). Although most individual floods produced erosion-dominated responses, the cumulative change between 2018 and 2024 was characterised by net sediment storage and channel aggradation, with approximately 93% of the reach experiencing deposition and only 7% erosion (Sheikh et al., in press). Individual floods therefore maintained short-term geomorphic activity without determining the long-term trajectory of the channel. Similar behaviour has been reported in regulated rivers where repeated experimental floods primarily redistribute sediment stored within the channel rather than generate sustained net sediment export (Hashemi et al., 2024; Schmidt & Grams, 2011).

This contrast between event-scale and multi-year responses highlights the dominant role of sediment supply between floods. If experimental releases were the principal control, repeated erosion-dominated events would be expected to cause progressive channel degradation. Instead, persistent aggradation indicates that sediment supplied during inter-flood periods equalled or exceeded the volume exported during flood releases. Previous studies have identified the Ova da Cluozza as a major sediment source whose contributions can replenish channel storage between successive floods (Bertoldi et al., 2025; Sheikh et al., in press). A comparable contrast was observed for channel width: widening during individual floods was modest, whereas cumulative widening over 2018–2024 was substantially greater than the sum of discrete event responses (Sheikh et al., in press). Long-term channel evolution therefore reflects the combined effects of experimental floods, tributary sediment delivery, intervening flows and progressive bank adjustment.

These findings demonstrate that geomorphic effectiveness should not be evaluated solely on the basis of the immediate response to individual flood releases. Instead, it should be considered an emergent property arising from interactions among flood characteristics, antecedent channel conditions, sediment availability, and tributary connectivity, operating across multiple timescales. For sediment-rich regulated rivers such as the lower Spöl, environmental flow design should adopt a sediment-aware approach that explicitly accounts for tributary sediment supply when defining flood magnitude, duration, and frequency. Such strategies would improve the ability of experimental floods to achieve long-term geomorphic and ecological objectives while maintaining channel dynamism and habitat heterogeneity. Future research should therefore integrate geomorphic monitoring between successive floods with sediment transport measurements and numerical modelling to quantify tributary contributions and evaluate how flood sequencing and sediment supply jointly control channel evolution.

These findings suggest that environmental-flow effectiveness should be evaluated over the long term rather than from the immediate response to individual releases. In sediment-rich regulated rivers, flood magnitude alone is unlikely to determine whether the channel degrades, aggrades or maintains morphological diversity. Environmental-flow design should therefore account for the timing and magnitude of sediment inputs, the degree of sediment recharge since the preceding effective event, and the capacity of a release to redistribute or export that material. Flood magnitude, duration, and frequency may need to be adjusted in relation to tributary connectivity and antecedent sediment availability rather than prescribed as fixed hydraulic targets. Future research should prioritise monitoring geomorphic adjustment and sediment replenishment during inter-flood

https://doi.org/10.5194/egusphere-2026-6858
Preprint. Discussion started: 12 November 2026
© Author(s) 2026. CC BY 4.0 License.

periods, because these intervals can substantially modify sediment availability, bed structure and the initial channel conditions encountered by the next experimental flood release. Integrating inter-flood observations with event-scale analyses of individual experimental floods would provide a more continuous understanding of sediment transfer and channel adjustment, clarify how short-term responses accumulate into long-term channel evolution, and improve understanding of the system as a whole. Numerical modelling tools could then build on this process-based evidence to test alternative flood magnitudes, durations, hydrograph shapes and sequences under varying sediment-supply conditions, thereby supporting more reliable prediction and design of experimental flows.

6 Conclusion

This study demonstrates that experimental floods in the lower Spöl River consistently reactivated geomorphic processes, but their effects varied markedly among events. Differences in sediment mobilisation, erosion and deposition, channel widening, grain-size change, roughness and slope could not be explained by any single hydrograph characteristic. Instead, geomorphic response emerged from the interaction between hydraulic forcing and the inherited channel state, including sediment availability, bed-surface condition, initial morphology, intervening flows and the legacy of preceding floods.

A key contribution of this study is its integrated assessment of six sequential floods using multiple hydrograph descriptors, initial conditions and complementary geomorphic response metrics. This multi-event, multi-metric framework distinguished between vertical reworking, lateral adjustment, sediment sorting and bed restructuring, revealing that these components were only partly coupled. Analysing the floods as a sequence further exposed channel-memory effects and evolving antecedent conditions that would have remained obscured if each event had been evaluated independently.

The results also show that event-scale effectiveness does not necessarily determine long-term channel evolution. Although individual releases frequently produced erosion-dominated responses, continued sediment delivery from the Ova da Cluozza promoted net aggradation and sediment storage over multiple years. Environmental-flow design in sediment-influenced regulated rivers should therefore move beyond fixed discharge targets and explicitly consider sediment supply, tributary connectivity, antecedent channel conditions and flood sequencing. Integrating event-scale monitoring with inter-flood assessment and numerical modelling would support more reliable prediction and adaptive design of experimental flows. More broadly, the framework developed here provides a transferable approach for evaluating environmental-flow programmes where long-term channel evolution depends on the interaction between flow releases, sediment connectivity and channel memory.

https://doi.org/10.5194/egusphere-2026-6858
Preprint. Discussion started: 12 November 2026
© Author(s) 2026. CC BY 4.0 License.

Appendix A: Analysis extent and experimental flood characteristics

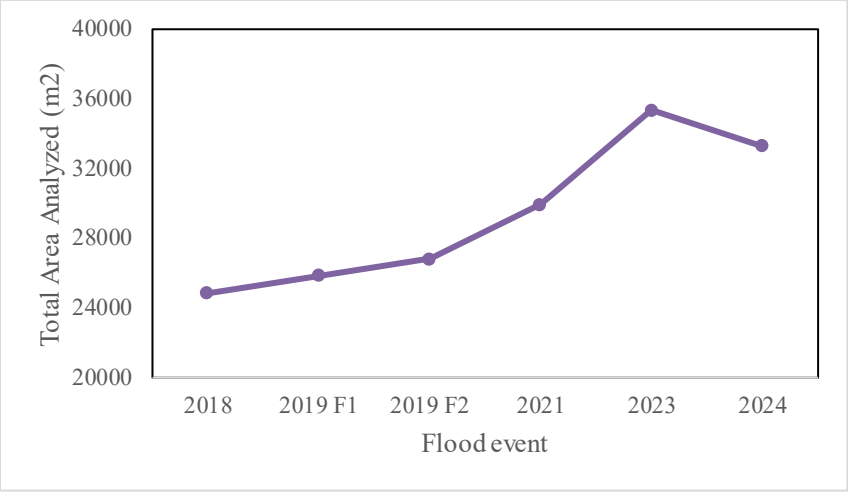


Figure A 1: Total channel area analyzed for each experimental flood event between 2018 and 2024.

Table A 1: Hydrological characteristics of the experimental floods conducted between 2018 and 2024.

Date	Released peak discharge (m^3/s)	Total Duration (h)	Peak duration (h)	Rising/falling duration Ratio (-)	Rising limb duration (h)	Falling limb duration (h)	Input: Ova da Cluozza (m^3/s)	Total volume released (m^3)
2018.09.04	25.9	8	2	0.5	2.25	4.5	0.93	430200
2019.06.19	25.9	9	1.5	0.75	3.21	4.29	2.6	486360
2019.06.24	40.9	12	1.75	1.25	5.69	4.56	2.3	950490
2020.07.01	25.9	10	1.5	1.25	4.72	3.78	1.77	515160
2021.06.23	25.9	10	1.5	1.29	4.79	3.71	2.7	515160
2023.06.15	25.9	19	4.5	0.88	6.79	7.71	1.2	904410
2024.06.11	24.9	16	2 peaks of 2.75 h and 2 h each	peak 1: 3; peak 2: 0.1	peak 1: 5.25; peak 2: 0.75 2.25	peak 1: 1.75; peak 2: 7 2.5	3.16	835830

https://doi.org/10.5194/egusphere-2026-6858
Preprint. Discussion started: 12 November 2026
© Author(s) 2026. CC BY 4.0 License.

Appendix B: Supplementary Geomorphic Analysis

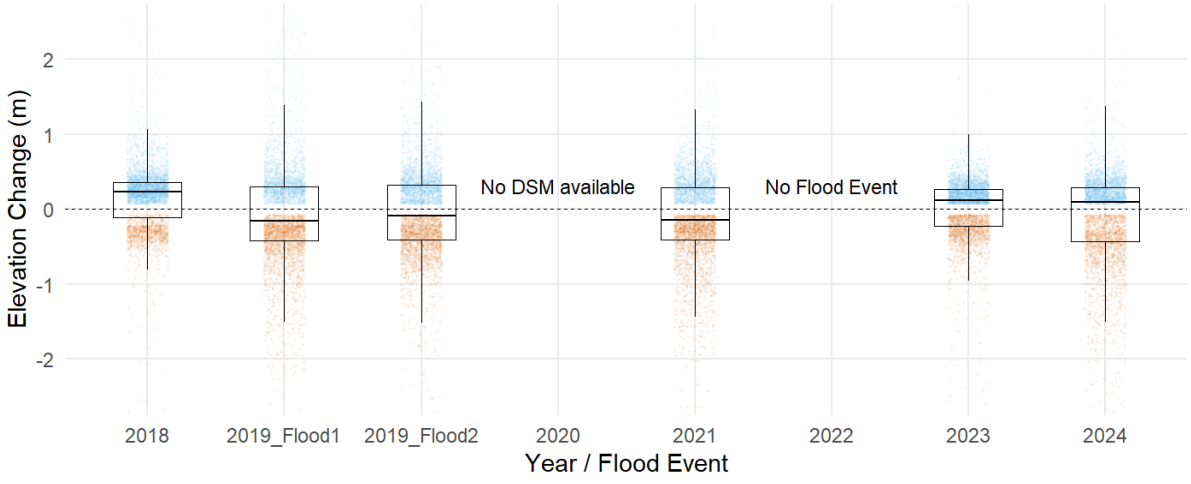


Figure B 1: Boxplots showing interquartile ranges of elevation changes across six flood events

780

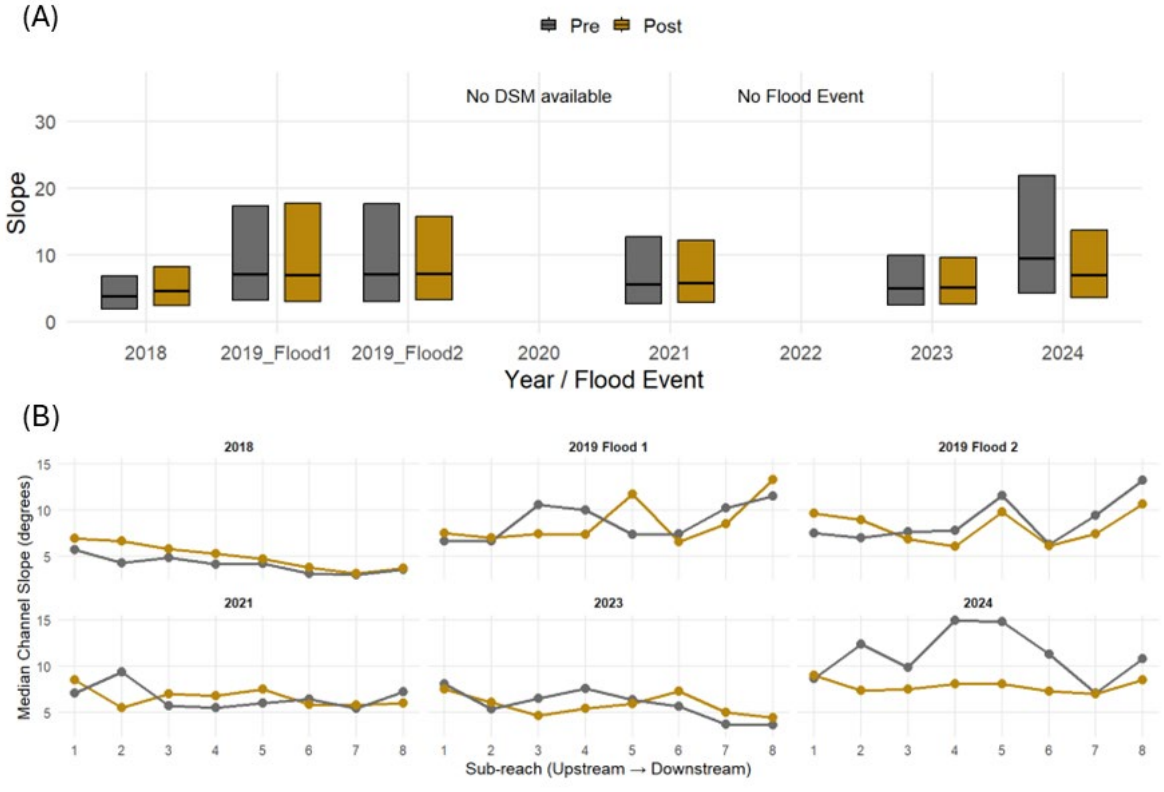


Figure B 2: Pre- (grey) and post-flood (yellow) channel slope: (A) overall distributions and (B) median values across eight sub-reaches. No DSM was available for 2020, and no experimental flood occurred in 2022.

https://doi.org/10.5194/egusphere-2026-6858
Preprint. Discussion started: 12 November 2026
© Author(s) 2026. CC BY 4.0 License.

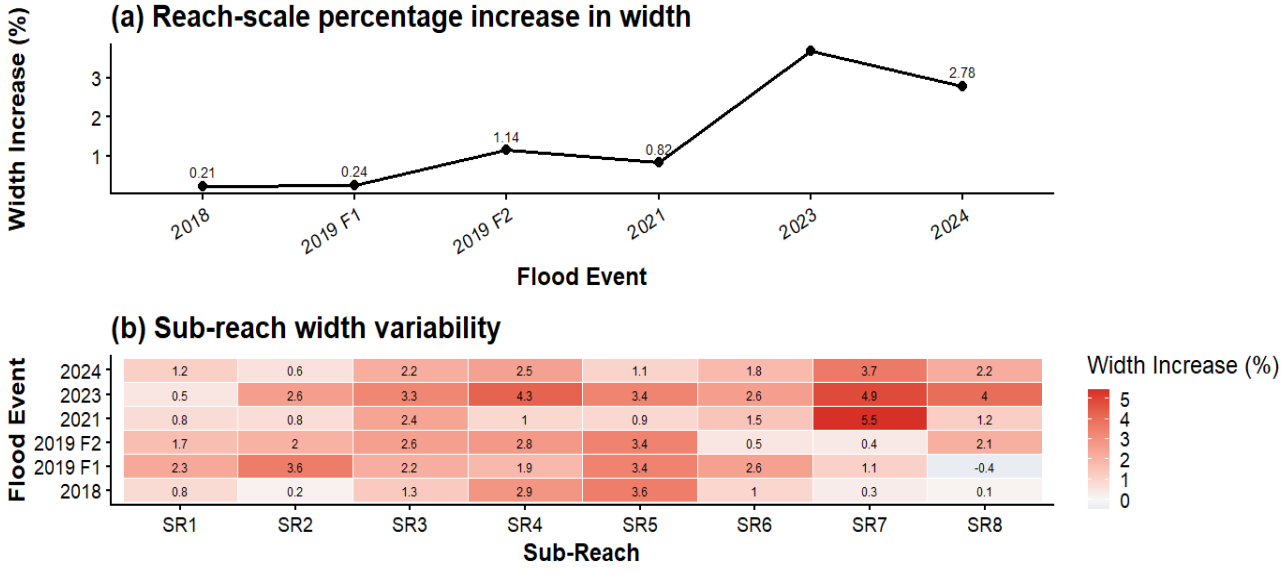


Figure B 3: Channel width response to flood events from 2018 to 2024 at reach and sub-reach scales. (a) Reach-scale percentage increase in channel width for each flood event. (b) Spatial variability in width increase (%) across sub-reaches (SR1–SR8) for each event, illustrating downstream heterogeneity in channel widening.

Appendix C: Relationships between pre-flood grain size and sediment mobilization

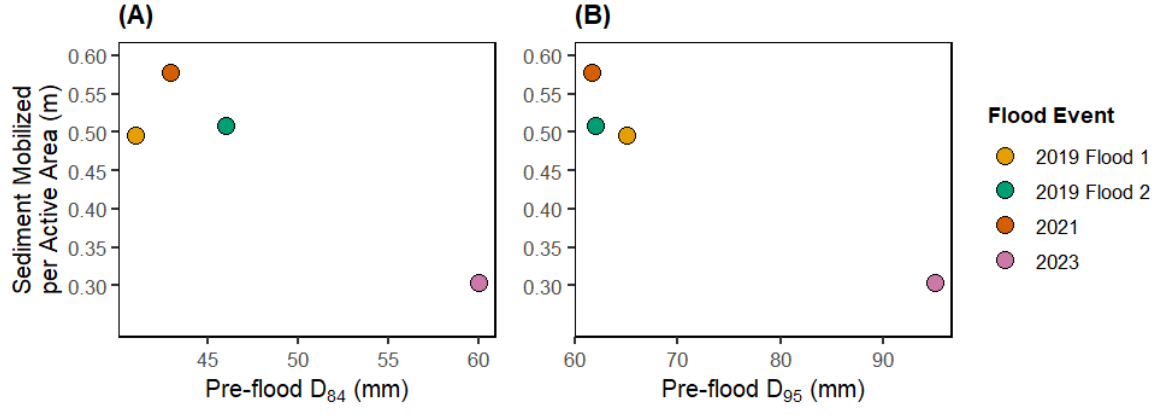


Figure C 1: Relationships between sediment mobilization per active area and the pre-flood coarser grain-size fractions: (A) D_{84} and (B) D_{95}. Colours indicate individual flood events. The 2018 and 2024 events are excluded because D_{84} and D_{95} measurements were unavailable.

https://doi.org/10.5194/egusphere-2026-6858
Preprint. Discussion started: 12 November 2026
© Author(s) 2026. CC BY 4.0 License.

Author contributions

MS: Conceptualization, Methodology, Formal analysis, Investigation, Data curation, Visualization, Writing – original draft, Writing – review & editing. **VRV:** Conceptualization, Methodology, Supervision, Funding acquisition, Writing – review & editing. **SW:** Data curation. **PP:** Supervision, Writing – review & editing.

Competing interests

The authors declare no competing interests.

Data availability

The processed data supporting the findings of this study are publicly available in the Mendeley Data repository (Sheikh and Ruiz-Villanueva, 2026; https://doi.org/10.17632/4r4j7kk72t.1).

Acknowledgements

This study has been partially supported by the University of Bern (UniBE), the University of Lausanne (UNIL), the Swiss National Science Foundation (PCEFP2_186963), and the Research Commission of the Swiss National Park (SNP-FOK) of the Swiss Academy of Sciences (SCNAT). We thank Engadiner Kraftwerke for implementing the e-floods each year and providing the released discharge data. We especially thank Stefanie Gubler (SCNAT), Ruedi Haller (SNP), and Simon Aeschbacher (SNP) for their support.

Financial support

This work was supported by the University of Bern, Switzerland, the University of Lausanne (UNIL), the Swiss National Science Foundation (PCEFP2_186963), and the Research Commission of the Swiss National Park (SNP-FOK) of the Swiss Academy of Sciences (SCNAT).

https://doi.org/10.5194/egusphere-2026-6858
Preprint. Discussion started: 12 November 2026
© Author(s) 2026. CC BY 4.0 License.

References

Bailey, P., Wheaton, J. M.;, Reimer, M., and Brasington, J.: Geomorphic Change Detection Software, https://doi.org/https://doi.org/10.5281/zenodo.7248344, 2020., 2020.

Beilfuss, R.: Prescribed Flooding and Restoration Potential in the Zambezi Delta, Mozambique, Zambezi Basin Crane and Wetland Conservation Program, https://doi.org/10.13140/RG.2.2.24321.45924, 2001.

Bender, I., Pittock, J., and Roberts, J.: Snowy River environmental flows post-2002: Lessons to be learnt, Mar. Freshw. Res., 73, 454–468, https://doi.org/10.1071/MF21209, 2022.

Bertoldi, W., Schiavi Cappello, N., and Soto Parra, T.: Aggradation and Widening in a Dam-Regulated Alpine River Aggradation and Widening in a Dam-Regulated Alpine River, in: Proceedings of the I.S. Rivers 2025 Conference, https://hal.science/hal-05169933v1, 2025.

Brasington, J., Langham, J., and Rumsby, B.: Methodological sensitivity of morphometric estimates of coarse fluvial sediment transport, Geomorphology, 53, 299–316, https://doi.org/10.1016/S0169-555X(02)00320-3, 2003.

Buraas, E. M., Renshaw, C. E., Magilligan, F. J., and Dade, W. B.: Impact of reach geometry on stream channel sensitivity to extreme floods, Earth Surf. Process. Landf., 39, 1778–1789, https://doi.org/10.1002/esp.3562, 2014.

Church, M.: Bed material transport and the morphology of alluvial river channels, Annu. Rev. Earth Planet. Sci., 34, 325–354, https://doi.org/10.1146/annurev.earth.33.092203.122721, 2006.

Consoli, G., Haller, R. M., Doering, M., Hashemi, S., and Robinson, C. T.: Tributary effects on the ecological responses of a regulated river to experimental floods, J. Environ. Manage., 303, https://doi.org/10.1016/j.jenvman.2021.114122, 2022.

Dazzi, N.: Quantification of geomorphological changes due to experimental floods in the Spöl river, Bachelor's thesis, University of Bern, Bern, https://www.parcs.ch/snp/mmd_fullentry.php?docu_id=55766&utm, 2024.

Dietrich, William. E., Kirchner, James. W., Ikeda, Hiroshi., and Iseya, F.: Sediment supply and the development of the coarse surface layer in gravel-bedded rivers, Nature, 340, 215–217, https://doi.org/10.1038/340215a0, 1989.

Eltner, A., Kaiser, A., Castillo, C., Rock, G., Neugirg, F., and Abellán, A.: Image-based surface reconstruction in geomorphometry - merits, limits and developments, Earth Surface Dynamics, 4, 359–389, https://doi.org/10.5194/esurf-4-359-2016, 2016.

Essyad, K., Samora, I., Delaloye, C., and Meile, C. T.: Multi-factor approach for bedload restoration of dam impacted rivers application to the Sarine river Multi-factor approach for bedload restoration of dam impacted rivers, application to the Sarine river, in: Proceedings of the 10th International Symposium on Hydraulic Structures (ISHS 2024), 821–830, https://doi.org/10.3929/ethz-b-000676028, 2024.

Federal Office for the Environment (FOEN): Ova da Cluozza- Zernez Station 2319, https://www.hydrodaten.admin.ch/en/seen-und-fluesse/stations/2319, last access: 1 July 2024., 2024.

https://doi.org/10.5194/egusphere-2026-6858
Preprint. Discussion started: 12 November 2026
© Author(s) 2026. CC BY 4.0 License.

Finch, B. D., Gibaja del Hoyo, J., Aarnink, J. L., O'Callaghan, M., and Ruiz-Villanueva, V.: Monitoring the Large Wood Regime in a Partially Regulated Alpine River Following Several Experimental Floods, Water Resour. Res., 61, https://doi.org/10.1029/2024WR038921, 2025.

Gaeuman, D., Stewart, R., Schmandt, B., and Pryor, C.: Geomorphic response to gravel augmentation and high-flow dam release in the Trinity River, California, Earth Surf. Process. Landf., 42, 2523–2540, https://doi.org/10.1002/esp.4191, 2017.

Galay, V. J.: Causes of river bed degradation, Water Resour. Res., 19, 1057–1090, https://doi.org/10.1029/WR019i005p01057, 1983.

GDAL/OGR contributors: GDAL Geospatial Data Abstraction Library, https://doi.org/10.5281/zenodo.5884351, 2024., 2024.

Gervasi, A. A., Pasternack, G. B., and East, A. E.: Flooding duration and volume more important than peak discharge in explaining 18 years of gravel–cobble river change, Earth Surf. Process. Landf., 46, 3194–3212, https://doi.org/10.1002/esp.5230, 2021.

Graf, W. L.: Downstream hydrologic and geomorphic effects of large dams on American rivers, Geomorphology, 79, 336–360, https://doi.org/10.1016/j.geomorph.2006.06.022, 2006.

Gräler, B., Van Den Berg, M. J., Vandenberghe, S., Petroselli, A., Grimaldi, S., De Baets, B., and Verhoest, N. E. C.: Multivariate return periods in hydrology: A critical and practical review focusing on synthetic design hydrograph estimation, https://doi.org/10.5194/hess-17-1281-2013, 2013., 2013.

Grant, G. E., Schmidt, J. C., and Lewis, S. L.: A Geologic Framework for Interpreting Geomorphic Effects of Dams, in: A Peculiar River: Geology, Geomorphology, and Hydrology of the Deschutes River, Oregon, vol. 7, edited by: O'Connor, J. E. and Grant, G. E., American Geophysical Union, Washington, DC, 209–225, https://doi.org/https://doi.org/10.1029/007WS13, 2003.

Gupta, A. and Fox, H.: Effects of high-magnitude floods on channel form: A case study in Maryland Piedmont, Water Resour. Res., 10, 499–509, https://doi.org/10.1029/WR010i003p00499, 1974.

Hashemi, S., Carrivick, J., and Klaar, M.: Hydromorphological response of heavily modified rivers to flood releases from reservoirs: A case study of the Spöl River, Switzerland, Earth Surf. Process. Landf., 49, 1028–1046, https://doi.org/10.1002/esp.5749, 2024.

International Commission on Large Dams (ICOLD): World Register of Dams – General synthesis, https://www.icold-cigb.org/GB/world_register/world_register_of_dams.asp, last access: 24 July 2025., 2025.

James, M. R., Chandler, J. H., Eltner, A., Fraser, C., Miller, P. E., Mills, J. P., Noble, T., Robson, S., and Lane, S. N.: Guidelines on the use of structure-from-motion photogrammetry in geomorphic research, Earth Surf. Process. Landf., 44, 2081–2084, https://doi.org/10.1002/esp.4637, 2019.

Jen, W. H. and Chen, Y. C.: Photogrammetric reconstruction of multi-decadal topographic changes from historical aerial imagery for landslide and debris-flow hazard assessment, Remote Sens. Appl., 41, 101866, https://doi.org/10.1016/j.rsase.2025.101866, 2026.

https://doi.org/10.5194/egusphere-2026-6858
Preprint. Discussion started: 12 November 2026
© Author(s) 2026. CC BY 4.0 License.

Junk, W. J., Bayley, P. B., and Sparks, R. E.: The Flood Pulse Concept in River-Floodplain Systems, in: Proceedings of the International Large River Symposium (LARS), edited by: Dodge, D. P., Canadian Special Publication of Fisheries and Aquatic Sciences, 106, 110–127, https://www.waterboards.ca.gov/bay_delta/docs/cmnt081712/sldmwa/junketal1989.pdf?utm, 1989.

Kingsford, R. T., Bino, G., and Porter, J. L.: Continental impacts of water development on waterbirds, contrasting two Australian river basins: Global implications for sustainable water use, Glob. Chang. Biol., 23, 4958–4969, https://doi.org/10.1111/gcb.13743, 2017.

Kondolf, G. M. and Swanson, M. L.: Channel adjustments to reservoir construction and gravel extraction along Stony Creek, California, Environmental Geology, 21, 256–269, https://doi.org/10.1007/BF00775916, 1993.

Konrad, C. P., Olden, J. D., Lytle, D. A., Melis, T. S., Schmidt, J. C., Bray, E. N., Freeman, M. C., Gido, K. B., Hemphill, N. P., Kennard, M. J., McMullen, L. E., Mims, M. C., Pyron, M., Robinson, C. T., and Williams, J. G.: Large-scale flow experiments for managing river systems, Bioscience, 61, 948–959, https://doi.org/10.1525/bio.2011.61.12.5, 2011.

Lane, S. N., Gaillet, T., and Goldenschue, L.: Restoring morphodynamics downstream from Alpine dams: Development of a geomorphological version of the serial discontinuity concept, Geomorphology, 402, https://doi.org/10.1016/j.geomorph.2022.108131, 2022.

Ligon, F. K., Dietrich, W. E., and Trush, W. J.: Downstream Ecological Effects of Dams, BioScience, 45, 183–192, https://doi.org/10.2307/1312557, 1995.

Lisle, T. E. and Church, M.: Sediment transport-storage relations for degrading, gravel bed channels, Water Resour. Res., 38, 1219, https://doi.org/10.1029/2001wr001086, 2002.

Loire, R., Piégay, H., Malavoi, J. R., Kondolf, G. M., and Bêche, L. A.: From flushing flows to (eco)morphogenic releases: evolving terminology, practice, and integration into river management, Earth. Sci. Rev., 213, 103475, https://doi.org/10.1016/j.earscirev.2020.103475, 2021.

Lu, D., Mausel, P., Brondízio, E., and Moran, E.: Change detection techniques, Int. J. Remote Sens., 25, 2365–2401, https://doi.org/10.1080/0143116031000139863, 2004.

Madej, M. A., Sutherland, D. G., Lisle, T. E., and Pryor, B.: Channel responses to varying sediment input: A flume experiment modeled after Redwood Creek, California, Geomorphology, 103, 507–519, https://doi.org/10.1016/j.geomorph.2008.07.017, 2009.

Magdaleno, F.: Experimental floods: A new era for Spanish and Mediterranean rivers?, Environ. Sci. Policy, 75, 10–18, https://doi.org/10.1016/j.envsci.2017.05.011, 2017.

Magilligan, F. J., Buraas, E. M., and Renshaw, C. E.: The efficacy of stream power and flow duration on geomorphic responses to catastrophic flooding, Geomorphology, 228, 175–188, https://doi.org/10.1016/j.geomorph.2014.08.016, 2015.

Mulligan, M., Lehner, B., Zarfl, C., Thieme, M., Beames, P., van Soesbergen, A., Higgins, J., Januchowski-Hartley, S. R., Brauman, K. A., De Felice, L., Wen, Q., Garcia de Leaniz, C., Belletti, B., Mandle, L., Yang, X., Wang, J., and Mazany-Wright, N.: Global Dam Watch: curated data and tools for management and decision making, https://doi.org/10.1088/2634-4505/ac333a, 1 December 2021., 2021.

https://doi.org/10.5194/egusphere-2026-6858
Preprint. Discussion started: 12 November 2026
© Author(s) 2026. CC BY 4.0 License.

Neverman, A. J., Fuller, I. C., and Procter, J. N.: Application of Geomorphic Change Detection (GCD) to quantify morphological budgeting error in a New Zealand gravel-bed river: a case study from the Makaroro River, Hawke's Bay, Journal of Hydrology (New Zealand), 55, 45–63, https://www.jstor.org/stable/43945085, 2016.

O'Callaghan, M., del Hoyo, J. G., Finch, B. D., and Ruiz-Villanueva, V.: Grow With the Flow? Impact of Experimental Floods on Riparian Vegetation in an Alpine River, River Res. Appl., https://doi.org/10.1002/rra.70044, 2025.

Olden, J. D., Konrad, C. P., Melis, T. S., Kennard, M. J., Freeman, M. C., Mims, M. C., Bray, E. N., Gido, K. B., Hemphill, N. P., Lytle, D. A., McMullen, L. E., Pyron, M., Robinson, C. T., Schmidt, J. C., and Williams, J. G.: Are large-scale flow experiments informing the science and management of freshwater ecosystems?, Front. Ecol. Environ., 12, 176–185, https://doi.org/10.1890/130076, 2014.

Patten, D. T., Harpman, D. A., Voita, M. I., and Randle, T. J.: A managed flood on the Colorado River: Background, objectives, design, and implementation, Ecological Applications, 11, 635–643, https://doi.org/10.1890/1051-0761(2001)011[0635:AMFOTC]2.0.CO;2, 2001.

Pellegrini, G., Martini, L., Rainato, R., and Picco, L.: Large wood mobilization and morphological changes in an alpine river following the release of an ordinary experimental flood from an upstream dam, Catena (Amst)., 216, 106398, https://doi.org/10.1016/j.catena.2022.106398, 2022.

Peppa, M. V., Mills, J. P., Moore, P., Miller, P. E., and Chambers, J. E.: Automated co-registration and calibration in SfM photogrammetry for landslide change detection, Earth Surf. Process. Landf., 44, 287–303, https://doi.org/10.1002/esp.4502, 2019.

Phillips, C. B., Hill, K. M., Paola, C., Singer, M. B., and Jerolmack, D. J.: Effect of Flood Hydrograph Duration, Magnitude, and Shape on Bed Load Transport Dynamics, Geophys. Res. Lett., 45, 8264–8271, https://doi.org/10.1029/2018GL078976, 2018.

Pix4D SA: PIX4D Mapper, https://www.pix4d.com/?utm (last access: 4 November 2026)., n.d.

Poff, N. L. and Zimmerman, J. K. H.: Ecological responses to altered flow regimes: A literature review to inform the science and management of environmental flows, https://doi.org/10.1111/j.1365-2427.2009.02272.x, January 2010., 2010.

Rickenmann, D. and Recking, A.: Evaluation of flow resistance in gravel-bed rivers through a large field data set, Water Resour. Res., 47, https://doi.org/10.1029/2010WR009793, 2011.

Righini, M., Surian, N., Wohl, E., Marchi, L., Comiti, F., Amponsah, W., and Borga, M.: Geomorphic response to an extreme flood in two Mediterranean rivers (northeastern Sardinia, Italy): Analysis of controlling factors, Geomorphology, 290, 184–199, https://doi.org/10.1016/j.geomorph.2017.04.014, 2017.

Robinson, C. T., Siebers, A. R., and Ortlepp, J.: Long-term ecological responses of the River Spöl to experimental floods, Freshwater Science, 37, 433–447, https://doi.org/10.1086/699481, 2018.

Ruiz-Villanueva, V., Aarnink, J. A., Gibaja, J., Finch, B., and Vuaridel, M.: Integrating flow-, sediment-and instream wood-regimes during e-flows in the Spöl River (Swiss Alps), in: Proceedings of the IAHR World Congress, 611–615, https://doi.org/https://doi.org/10.3850/IAHR-39WC2521711920221000?utm, 2022.

https://doi.org/10.5194/egusphere-2026-6858
Preprint. Discussion started: 12 November 2026
© Author(s) 2026. CC BY 4.0 License.

Ruiz-Villanueva, V., Piégay, H., Scorpio, V., Bachmann, A., Brousse, G., Cavalli, M., Comiti, F., Crema, S., Fernández, E., Furdada, G., Hajdukiewicz, H., Hunzinger, L., Lucía, A., Marchi, L., Moraru, A., Piton, G., Rickenmann, D., Righini, M., Surian, N., Yassine, R., and Wyżga, B.: River widening in mountain and foothill areas during floods: Insights from a meta-analysis of 51 European Rivers, Science of the Total Environment, 903, https://doi.org/10.1016/j.scitotenv.2023.166103, 2023.

Ruiz-Villanueva, V., Sheikh, M., Aarnink, J., Finch, B., Del Hoyo Gibaja, J., O'Callaghan, M., and Consoli, G.: River sediment grain size and sorting changes after several experimental floods in the lower Spöl River (Switzerland), J. Soils Sediments, 26, https://doi.org/https://doi.org/10.1007/s11368-026-04490-8, 2026.

Scheurer, T. and Molinari, P.: Experimental floods in the River Spöl, Swiss National Park: Framework, objectives and design, https://doi.org/10.1007/s00027-003-0667-4, 2003.

Schläfli, S.: Regulated flows influence on river morphodynamics: The Spöl River (Swiss National Park), Master's Thesis, University of Bern, Switzerland, https://www.parcs.ch/snp/pdf_public/2022/37650_20220818_100253_MScThesis_SalomeSchlaefli.pdf, 2018.

Schmidt, J. C. and Grams, P. E.: The high Flows-Physical Science Results, in: Effects of Three High-Flow Experiments on the Colorado River Ecosystem Downstream from Glen Canyon Dam, Arizona, edited by: Melis, T. S., U.S. Geological Survey, 53–92, https://doi.org/https://doi.org/10.3133/cir1366, 2011.

Schmidt, J. C. and Wilcock, P. R.: Metrics for assessing the downstream effects of dams, Water Resour. Res., 44, W04404, https://doi.org/10.1029/2006WR005092, 2008.

Sheikh, M., Weismann, S., and Ruiz-Villanueva, V.: Exploring the Recent Morphological Evolution and Effectiveness of Seven Experimental Floods In the Lower Spöl River (Swiss Alps), in: IAHR 13th International Conference on Fluvial Hydraulics - River flow 2026, 2026.

Smith, V. B. and Mohrig, D.: Geomorphic signature of a dammed Sandy River: The lower Trinity River downstream of Livingston Dam in Texas, USA, Geomorphology, 297, 122–136, https://doi.org/10.1016/j.geomorph.2017.09.015, 2017.

Soto Parra, T., Politti, E., and Zolezzi, G.: Morphological and fish mesohabitat dynamics following an experimental flood under different sediment availability, Earth Surf. Process. Landf., 49, 5167–5185, https://doi.org/10.1002/esp.6025, 2024.

Stähly, S., Franca, M. J., Robinson, C. T., and Schleiss, A. J.: Sediment replenishment combined with an artificial flood improves river habitats downstream of a dam, Sci. Rep., 9, https://doi.org/10.1038/s41598-019-41575-6, 2019.

Sumitomo, K., Watanabe, Y., Izumi, N., Yamaguchi, S., and Yokohama, H.: Study on The Effects Of Artificial Flood For River Channel Disturbance In The Maintenance Of Old Watercourses, Journal of Japan Society of Civil Engineers, 6, https://doi.org/https://doi.org/10.2208/journalofjsce.6.1_69, 2018.

Venditti, J. G., Nelson, P. A., Minear, J. T., Wooster, J., and Dietrich, W. E.: Alternate bar response to sediment supply termination, J. Geophys. Res. Earth Surf., 117, F02039, https://doi.org/10.1029/2011JF002254, 2012.

Vericat, D. and Batalla, R. J.: Sediment transport in a large impounded river: The lower Ebro, NE Iberian Peninsula, Geomorphology, 79, 72–92, https://doi.org/10.1016/j.geomorph.2005.09.017, 2006.

https://doi.org/10.5194/egusphere-2026-6858
Preprint. Discussion started: 12 November 2026
© Author(s) 2026. CC BY 4.0 License.

Westoby, M. J., Brasington, J., Glasser, N. F., Hambrey, M. J., and Reynolds, J. M.: "Structure-from-Motion" photogrammetry: A low-cost, effective tool for geoscience applications, Geomorphology, 179, 300–314, https://doi.org/10.1016/j.geomorph.2012.08.021, 2012.

Wheaton, J. M., Brasington, J., Darby, S. E., and Sear, D. A.: Accounting for uncertainty in DEMs from repeat topographic surveys: Improved sediment budgets, Earth Surf. Process. Landf., 35, 136–156, https://doi.org/10.1002/esp.1886, 2010.

Williams, Garnett. P. and Wolman, M. G.: Downstream Effects of Dams of Alluvial Rivers, Washington, DC, https://doi.org/https://doi.org/10.3133/pp1286, 1984.

Williams, R. D.: DEMs of Difference, in: Geomorphological Techniques, edited by: Cook, S. J., Clarke, L. E., and Nield, J. M., British Society for Geomorphology, 2, Sect. 3.2, 1–17, https://eprints.gla.ac.uk/114527/, 2012.

Wohl, E.: Messy rivers are healthy rivers: The implications of physical complexity for river ecosystems www.globalwaterforum.org/2016/10/31/messy-rivers-are-healthy-rivers-the-implications-of-physical-complexity-for-river-ecosystems, 2016.

Wolman, M. G.: A method of sampling coarse river-bed material, Eos, Transactions American Geophysical Union, 35, 951–956, https://doi.org/10.1029/TR035i006p00951, 1954.

Wolman, M. G. and Miller, J. P.: Magnitude and Frequency of Forces in Geomorphic Processes, J. Geol., 68, 54–74, https://doi.org/10.1086/626637, 1960.

Yager, E. M., Dietrich, W. E., Kirchner, J. W., and McArdell, B. W.: Prediction of sediment transport in step-pool channels, Water Resour. Res., 48, W01541, https://doi.org/10.1029/2011WR010829, 2012.

Yamaguchi, S., Watanabe, Y., Takahashi, T., and Sumitomo, K.: Effective Excavation For Restoring The Former Watercourses Of A River Where The Watercourses Are Established, in: 1th International Symposium on Ecohydraulics (ISE 2016),Melbourne, Australia, Paper No. 25936, https://ise-2016.m.asnevents.com.au/schedule/session/8117/abstract/25936, 2016.